Journal of Biological Systems, Vol. 28, No. 1 (2020) 1–40

DOI: 10.1142/S0218339020500060

THE EFFECTS OF INVASIVE EPIBIONTS ON CRAB–MUSSEL COMMUNITIES: A THEORETICAL APPROACH TO UNDERSTAND MUSSEL POPULATION DECLINE

JINGJING LYU*,¶, LINDA A. AUKER†, ANUPAM PRIYADARSHI‡ and RANA D. PARSHAD§

*College of Information Science and Engineering
Chengdu University, Chengdu, Sichuan Province, P. R. China

†Department of Biology
Misericordia University
Dallas, PA 18612, USA

‡Department of Mathematics
Institute of Science
Banaras Hindu University
Varanasi 221005, India

§Department of Mathematics
Iowa State University
Ames, Iowa 50011, USA
¶lvjingjing2014@outlook.com

Received 26 April 2019
Accepted 29 January 2020
Published 7 April 2020

Blue mussels (*Mytilus edulis*) are important keystone species that have been declining in the Gulf of Maine. This could be attributed to a variety of complex factors such as *indirect* effects due to invasion by epibionts, which remains unexplored mathematically. Based on classical optimal foraging theory (OFT) and anti-fouling defense mechanisms of mussels, we derive an ODE model for crab–mussel interactions in the presence of an invasive epibiont, *Didemnum vexillum*. The dynamical analysis leads to results on stability, global boundedness and bifurcations of the model. Next, via optimal control methods, we predict various ecological outcomes. Our results have key implications for preserving mussel populations in the advent of invasion by non-native epibionts. In particular, they help us understand the changing popluation dynamics of local predator–prey communities, due to indirect effects that epibionts confer.

Keywords: Predator–Prey System; Stability and Bifurcation; Optimal Control; Biological Invasion; Epibiont.

Mathematics Subject Classification 2020: Primary: 34C11, 34C23, 49J15; Secondary: 92D25, 92D40

¶Corresponding author.

1. Introduction

1.1. *Background*

Blue mussels (*Mytilus edulis*) are ecologically and economically important species.[1–3] They play several roles in marine ecosystems: as important prey for many species, such as crabs, shorebirds, sea stars, and gastropod molluscs[3–5]; as nutrient recyclers and pollution indicators[6]; and as a keystone species, serving as habitat for benthic infaunal organisms.[3,7] However, *M. edulis* has declined in the Gulf of Maine by over 60% since the 1970s.[8] Mussel post-larval settlement, consistent with this observation, has also declined.[9] The reasons for this decline are unclear, but are almost certainly complex. Thus, a clearer understanding of the ecological factors that influence mussel populations is needed.

A primary cause of a species population decline is predation. Invasive predators, like the green crab (*Carcinus maenas*) and the Asian shore crab (*Hemigrapsus sanguineus*), readily prey on the blue mussel.[10–12] However, mussel size limits crab predation, with crabs consuming mussel prey below 70 mm in shell length.[13] Furthermore, mussels have also adapted to crab predation by thickening their shells in response to novel predator presence, in extremely short time periods.[12] Furthermore, substrate complexity reduces predation on mussels as increasingly complex habitats provide refuge from crab predation.[15] Thus, while predation has put considerable pressure on mussel populations, rapidly evolving defense mechanisms, escape from predation via growth, and physical refuges have counteracted predator impacts.

Though mussels do have the aforementioned protections against predation, they are still in decline. Curiously, in the 1970s, an introduced ascidian species *Didemnum vexillum*, arrived in the Gulf of Maine.[16] *D. vexillum* is a colonial ascidian that is dominant as a competitor for substratum, prolifically laying down mat-like structures on any hard substrate.[17] Consequently, it acts as an epibiont (fouling organism) on *M. edulis*.[9,10] Epibionts impact predator–prey communities indirectly by affecting predation rates on basibionts. *D. vexillum* in particular has chemical anti-predatory defenses. If a crab predator attempts to break off pieces of the *D. vexillum* colony to reach the mussel, *D. vexillum* releases secondary metabolites and sulfuric acid that deters the crab.[17] This mechanism by which the epibiont protects the mussel from crab predation is known as associational resistance.[18] While it appears to protect mussels from crab predation, *D. vexillum* also negatively affects mussel fecundity and fitness, resulting in fewer progeny.[9] Thus, *D. vexillum* has both a positive and negative impact on mussel populations.

Given this complex relationship, we ask

- Could the introduced epibiont *D. vexillum* change the predator–prey dynamics in an established local crab–mussel community?
- Could the net effect of positive and negative impacts from *D. vexillum* epibiosis, lead to mussel population decline?

Our analysis is (to the best of our knowledge) the first mathematical investigation of predator–prey dynamics under pressure of fouling from epibionts in a crab–mussel community. Herein,

- we derive a predator–prey model for crab–mussel interactions, given that clearly a certain size of mussel is preferred or "optimal" for the crab,
- we consider the effects of an invasive epibiont by meshing Optimal Foraging Theory (OFT) and anti-fouling defense of the mussels,
- we model the effects of associational resistance and reduced fecundity, due to the epibiont, and
- we next investigate dynamical aspects of the model, and use optimal control theory to predict various outcomes.

In adult mussels, the protective periostracum, which inhibits epibiont settlement when present,[19] tends to wear off due to age, decay and abrasion. Consequently, the periostracum is more prevalent on newer regions of the shell, while absent on older regions.[20] This means juvenile mussels are less likely to be overgrown with epibionts than are adult mussels. When crabs forage for mussels, they typically prefer a medium-sized adult.[13,14] But this preferred size tends to get easily overgrown by epibionts. Epibionts can alter the prey size choice of predators, including crabs, in experiments,[17,21–23] though this has not yet been tested with *D. vexillum*. We hypothesize in this paper that *D. vexillum* can change the feeding preference of crabs away from mid-size adult mussels (that are easily overgrown and therefore less likely to be eaten) towards juvenile mussels (which are less likely to be overgrown and so are easier targets), even though the latter are not the crab's preferred food source. To elucidate our approach, we survey some classical results from OFT.

1.2. *Optimal foraging theory*

OFT predicts how animals behave when they forage for food. It is well known that predators optimize feeding strategies to maximize energy intake.[24] Essentially, predators try to gain the most energy from their prey by expending the least amount of energy in the hunting process. For a crab foraging for mussels, this amounts to maximizing

$$\frac{e}{h} = \frac{\text{energy gained from mussel intake}}{\text{handling time of mussel}}. \tag{1.1}$$

This translates to a medium-sized adult mussel as the optimally preferred prey by adult crabs. While large mussels have a potentially high source of energy, they take a much longer time to open and consume than smaller mussels. Small mussels, conversely, take a short time to consume, but they offer very little reward. Even so, juvenile mussels are readily consumed by many species, including green crabs and dogwhelk.[10]

We refer the reader to the mathematical treatment by Krivan,[25,26] who describes, via a three species ODE model, in which a predator hunts (optimally)

for two prey species u and v, where u is favored to v. The term u_1 denotes the attack rate with which prey u is hunted, and u_2 denotes the attack rate with which prey v is hunted. The analysis presented in Ref. 26 draws from classic results in OFT and shows that, in order to maximize $\frac{e}{h}$, the optimal pair of (u_1, u_2) is given by $u_1 = 1, u_2 = 0$ if $u > u^*$ or $u_1 = 1, u_2 = 1$ if $u < u^*$, or $u_1 = 1, 0 < u_2 < 1$ if $u = u^*$, where u^* is the critical density for switching.

1.2.1. *OFT in the presence of epibionts*

Predators are known to switch prey if preferred prey drop below a threshold density.[27] For example, fish species have been shown to switch habitats if foraging in one habitat becomes less fruitful than in another habitat.[28] Theoretical studies also support this.[25] In our context, if $\frac{e_1}{h_1} > \frac{e_2}{h_2}$, the adult mussels are preferred to juveniles as the optimal prey for crabs. If $\frac{e_1}{h_1} < \frac{e_2}{h_2}$, juveniles mussels are optimal to hunt.

Conjecture 1. *An increase in epibiont density will cause crabs to switch from adult mussels to juveniles even though the juvenile is less preferred and the adult mussel density remains high.*

Essentially, if one considers a predator–prey model with these species (crab–mussel-epibiont), there are two limiting cases

- There is no epibiont ($e = 0$), in this setting $\frac{e_1}{h_1} > \frac{e_2}{h_2}$, so $u_1 = 1, u_2 = 0$.
- The epibiont achieves its carrying capacity K, that is, $e = K$, in this setting, high epibiont density causes the handling time $h_1 \gg 1$, thus $\frac{e_1}{h_1} < \frac{e_2}{h_2}$, and so the crab switches to juveniles, and now $u_1 = 0, u_2 = 1$.

To this end, we first split the mussel class into adults and juveniles (we assume the juveniles have the protective periostracum whereas the adults do not). A crab species preying on two separate classes of adult and juveniles mussels (with adults being the preferred food type), places this in a classic one predator–two prey setting.[25] Based on the result we got in the experiment, shown in Fig. 1, our hypotheses for OFT are as follows:

(1) In the absence of epibionts, crab–mussel interactions follow classical OFT. That is, adult mussels will be attacked with rate 1, whilst the less preferred juveniles will not be attacked ($u_1 = 1, u_2 = 0$). We claim this is the only optimal strategy for the crab, as long as $d_1 > \frac{e_2}{h_2}$, where d_1 is the death rate of prey type 1.
(2) There is a change to the classical case, under pressure of epibiosis from *D. vexillum*.
(3) If a crab were to be presented with a preferred adult mussel overgrown with *D. vexillum*, it would switch to a prey of a less optimal size, even if the overall adult mussel density was high (assuming their was uniform overgrowing of all adult mussels).

Fig. 1. Classic crab preference (without epibiont) shown in left panel. Crabs were presented with clean and overgrown mussels,[9,10] and the handling times of the overgrown ones were up to 6 times greater than the clean ones (seen in center panel). These experimental results[9,10] lead us to conjecture that crabs will *switch* to the smaller uncovered juvenile mussels under pressure of epibiosis, shown in right panel.

(4) The switch would be to juvenile mussels, which we know are almost never overgrown because of their intact protective peristrocum. That is, in the ($e = K$) case, we have ($u_1 = 0, u_2 = 1$). We claim this is the only optimal strategy for the crab, as long as $d_1 > \frac{e_1}{h_1}$.
(5) This will in turn directly affect the feedback loop to the adult mussel population, given that juveniles are transitioning to adults.

The above is rigorously shown in Appendix (Sec. A.1).

2. Mathematical Formulation

Our goal is to derive a mathematical model that best captures our hypotheses. To this end, we make the following assumptions:

(1) An epibiont has invaded into a local crab–mussel community, and is growing logistically. It will eventually reach a critical carrying capacity.
(2) We model the pressure from epibiosis, in terms of the attack rates u_1, u_2. That is we assume these are *dependent on the epibiont density*. As a simple first approach, we assume

$$u_1(e) = \frac{K - e}{K}, \quad u_2(e) = \frac{e}{K}.$$

Thus, without any epibiont presence ($e = 0$), the adult mussel is the only prey eaten and the juvenile is not eaten at all because there is not enough energy gain for the effort involved, so $u_1 = 1, u_2 = 0$, in line with classical theory.[26] However, this starts to change as the epibiont starts to overgrow the mussels. When the epibiont is at carrying capacity, $e = K$, we assume the adult mussels are completely overgrown, and thus is not consumed at all. The crab switches completely to juveniles, so that $u_1 = 0$ and $u_2 = 1$.
(3) We model the decreasing fecundity in mussels due to epibiont cover by considering a growth rate $a = a(e)$. We consider $a = a(e) = a(\frac{K - \frac{e}{2}}{K})$. Hence, as epibionts get to carrying capacity $e = K$, this growth rate is cut in half and becomes $a/2$.

(4) We assume the intraspecies competition is present only in adult mussels, and not juveniles.[29]
(5) We assume the search rates λ_1 and λ_2 to be the same, and normalized to 1, so $\lambda_1 = \lambda_2 = 1$.

Based on the above assumptions, we have the following system of differential equations:

$$\frac{dC}{dt} = -d_1 C + e_1 u_1(e) \frac{M_A}{1 + h_1 u_1(e) M_A + h_2 u_2(e) M_J} C + e_2 u_2(e) \frac{M_J}{1 + h_1 u_1(e) M_A + h_2 u_2(e) M_J} C, \tag{2.1}$$

$$\frac{dM_A}{dt} = bM_J - \delta_1 M_A^2 - u_1(e) \frac{M_A}{1 + h_1 u_1(e) M_A + h_2 u_2(e) M_J} C, \tag{2.2}$$

$$\frac{dM_J}{dt} = a(e) M_A - bM_J - u_2(e) \frac{M_J}{1 + h_1 u_1(e) M_A + h_2 u_2(e) M_J} C, \tag{2.3}$$

$$\frac{de}{dt} = b_1 e \left(1 - \frac{e}{K}\right), \tag{2.4}$$

where

$$u_1(e) = \frac{K - e}{K}, \quad u_2(e) = \frac{e}{K}, \quad a(e) = a\left(\frac{K - \frac{e}{2}}{K}\right), \tag{2.5}$$

with positive initial conditions $C(0) = C_0, M_A(0) = M_{A0}, M_J(0) = M_{J0}, e(0) = e_0$. These responses are for the range $0 \leq e \leq K$.

Here, C, M_A and M_J are the densities of crabs, adult mussels and juvenile mussels population at a given time t, respectively. The population density of *D. vexillum* is e, while d_1 is the mortality rate of the crab, e_1 and e_2 are the energy gain to the crab from preying on the adult mussel and juvenile mussel, respectively, h_1 and h_2 are the handling time of the adult mussel and juvenile mussel, respectively, b is the rate at which juveniles leave the juvenile class and become adults, a is the rate at which juveniles are produced, δ_1 measures the intraspecific competition among adult mussels, b_1 is the intrinsic rate of growth of the epibiont population, and K is its carrying capacity.

3. Dynamical Analysis

3.1. *Boundedness*

We note from Eqs. (2.2) and (2.3), via positivity of solutions, standard comparison yields

$$\frac{dM_A}{dt} \leq bM_J - \delta_1 M_A^2, \tag{3.1}$$

$$\frac{dM_J}{dt} \leq aM_A - bM_J. \tag{3.2}$$

Integrating (3.2) in the time interval $[0,t]$ yields

$$M_J(t) \leq ae^{-bt}\int_0^t e^{bs}M_A(s)ds + e^{-bt}M_J(0) \leq a\int_0^t M_A(s)ds + M_J(0). \quad (3.3)$$

Now, similarly we can integrate (3.1) in the time interval $[0,t]$ to yield

$$C_0\delta_1\int_0^t M_A(s)ds \leq \delta_1\int_0^t (M_A(s))^2ds \leq b\int_0^t M_J(s)ds + M_A(0), \quad (3.4)$$

where C_0 is a constant. This follows via the embedding of $L^2[0,t] \hookrightarrow L^1[0,t]$. Next, we integrate (3.2) in the time interval $[0,t]$ to yield

$$b\int_0^t M_J(s)ds \leq a\int_0^t M_A(s)ds + M_J(0). \quad (3.5)$$

Using the estimate via (3.4) in (3.3) yields

$$M_J(t) \leq a\left(\frac{b}{c\delta_1}\int_0^t M_J(s)ds + \frac{1}{c\delta_1}M_A(0)\right) + M_J(0), \quad (3.6)$$

renaming parameters, we obtain

$$M_J(t) \leq C_1\int_0^t M_J(s)ds + C_2. \quad (3.7)$$

Thus, the integral version of Gronwall's lemma,[30] yields

$$M_J(t) \leq C_2(1 + C_1te^{C_1t}). \quad (3.8)$$

Now, since we have lower estimates on M_A via (3.3) and (3.5), this implies there exist constants C_3, C_4 s.t.

$$M_A(t) \geq C_3(te^{C_4t}). \quad (3.9)$$

For if not, we can assume $M_A(t) \leq C_3(te^{C_4t})$, choose appropriate C_3, C_4, and insert this estimate into (3.3), to derive a contradiction to the estimate for M_J.

Now note, the equation for e is bounded trivially by K. Addition of (2.1)–(2.3), and given the fact that $e_1 < 1$ and $e_2 < 1$, yields:

$$\frac{d(C + M_A + M_J)}{dt} \leq -d_1C + aM_A - \delta_1(M_A)^2. \quad (3.10)$$

Integrating the above equation in time, and using positivity of C yields

$$C + M_A + M_J + \delta_1\int_0^t (M_A(s))^2ds \leq a\int_0^t M_Ads + C(0) + M_A(0) + M_J(0). \quad (3.11)$$

We now use the upper and lower estimates on M_A via (3.9) and (3.4), yields

$$C + M_A + M_J + (C_3)^2\int_0^t s^2e^{C_42s}ds \leq a\int_0^t C_2(1 + C_1se^{C_1s})ds + C(0) + M_A(0) + M_J(0). \quad (3.12)$$

One sees that by choosing $[0,t]$ large enough, one can easily dominate $a\int_0^t C_2(1 + C_1te^{C_1t})ds$ by $(C_3)^2\int_0^t s^2e^{C_4s}ds$, no matter what the constants C_1, C_2, C_3, C_4 are.

This yields the ultimate dissipativity of the system. Essentially, this says, that for all time beyond some transition time, the state variables C, M_A and M_J are bounded, via a bound that depends only on the initial data, and parameters in the problem.

Thus, we can state the following theorem.

Theorem 3.1. *Consider the crab–mussel system* (2.1)–(2.4). *The solutions* (C, M_A, M_J, e), *satisfy the following uniform bounds for all times* $t > T^*$, *where* T^* *depends on the initial conditions and parameters in the problem.*

$$||C||_\infty \leq K_1, \quad ||M_A||_\infty \leq K_1, \quad ||M_J||_\infty \leq K_1, \quad ||e||_\infty \leq K_1, \tag{3.13}$$

for any initial conditions $(C(0), M_A(0), M_J(0), e(0)) \in L^\infty$.

Remark 1. Note, K_1 will depend on the initial conditions and various parameters in the problem. However, our focus is not to quantify how the bound K_1 depends on the various parameters in the problem, and/or initial conditions. Also note, our proof of ultimate dissipativity relies on choosing a large enough time interval $[0, t]$. However, for any intermediate finite time $t^* \in [0, t]$, M_A and M_J remain bounded via the estimates in (3.8) and (3.4). Thus, they can't blow-up in finite time. Now, C remains bounded for any intermediate time, easily seen by integrating (2.1), and using the earlier mentioned estimates for M_A, M_J.

3.2. *Equilibrium and local stability with no epibiont*

We now consider the existence and stability of the equilibrium for the system when there is no epibiont ($e = 0$). The system is simplified as

$$\frac{dC}{dt} = -d_1 C + e_1 \frac{M_A}{1 + h_1 M_A} C, \tag{3.14}$$

$$\frac{dM_A}{dt} = bM_J - \delta_1 M_A^2 - \frac{M_A}{1 + h_1 M_A} C, \tag{3.15}$$

$$\frac{dM_J}{dt} = aM_A - bM_J. \tag{3.16}$$

Two equilibria, $(0, 0, 0)$ and $(0, \frac{a}{\delta_1}, \frac{a^2}{\delta_1 b})$, on the boundary and one interior equilibrium (C^*, M_A^*, M_J^*). It is easy to see $(0, 0, 0)$ is unstable. And $(0, \frac{a}{\delta_1}, \frac{a^2}{\delta_1 b})$ is globally stable if $0 < e_1 - d_1 h_1 < \frac{d_1 \delta_1}{a}$ and unstable if $e_1 - d_1 h_1 > \frac{d_1 \delta_1}{a}$. The interior equilibrium is given by

$$C^* = \frac{e_1(a(e_1 - d_1 h_1) - d_1 \delta_1)}{(e_1 - d_1 h_1)^2}, \tag{3.17}$$

$$M_A^* = \frac{d_1}{e_1 - d_1 h_1}, \tag{3.18}$$

$$M_J^* = \frac{a d_1}{b(e_1 - d_1 h_1)}. \tag{3.19}$$

Note that $C^* > 0, M_A^* > 0$ and$M_J^* > 0$ if

$$e_1 - d_1 h_1 > \frac{d_1 \delta_1}{a}. \tag{3.20}$$

We next state the following theorem.

Theorem 3.2. *Consider the crab–mussel system* (2.1)–(2.4)*, without the presence of an epibiont, that is when* $e = 0$*. There exists an interior steady state* (C^*, M_A^*, M_J^*)*, which is locally asymptotically stable under the following criteria*:

$$\frac{d_1 \delta_1}{a} < e_1 - d_1 h_1 < \frac{d_1 \delta_1}{a} + \frac{d_1 \delta_1 e_1}{a h_1}, \quad d_1 > \frac{e_2}{h_2}. \tag{3.21}$$

The proof is relegated to Appendix (Sec. A.2).

Remark 2. Note, the second condition $d_1 > \frac{e_2}{h_2}$ is not a result of the Routh-Hurwitz criterion, rather it follows from Lemma A.1 in Sec. A.1. We enforce it so that the attack rates should be as predicted via classical OFT.

3.3. *Equilibrium and local stability analysis with epibiont*

Systems (2.1)–(2.4) have five possible equilibria. There is one in the interior of the positive octant (C^*, M_A^*, M_J^*, e^*), and four on the boundary, $(0, 0, 0, 0), (0, 0, 0, K), (0, \frac{a}{\delta_1}, \frac{a^2}{b\delta_1}, 0)$ and $(0, \frac{a}{2\delta_1}, \frac{a^2}{4b\delta_1}, K)$. It is easy to check that the equilibria with no epibiont, $(0, 0, 0, 0)$ and $(0, \frac{a}{\delta_1}, \frac{a^2}{b\delta_1}, 0)$, are unstable. Furthermore, $(0, \frac{a}{2\delta_1}, \frac{a^2}{4b\delta_1}, K)$ is stable if $0 < e_2 - d_1 h_2 < \frac{4bd_1\delta_1}{a^2}$ and unstable if $e_2 - d_1 h_2 > \frac{4bd_1\delta_1}{a^2}$. In fact, it is common that prey exist in a stable state in the absence of the predator. Finally, $(0, 0, 0, K)$ is also unstable. We will focus on the interior equilibrium.

Consider the interior equilibrium, i.e., (C^*, M_A^*, M_J^*, e^*). It is easy to see $e^* = K$ in the equilibrium state. Then we have $u_1(e^*) = 0, u_2(e^*) = 1, a(e^*) = \frac{a}{2}$. To get (C^*, M_A^*, M_J^*, e^*) explicitly, it is equivalent to solve the following equations:

$$-d_1 C + e_2 \frac{M_J}{1 + h_2 M_J} C = 0, \tag{3.22}$$

$$b M_J - \delta_1 M_A^2 = 0, \tag{3.23}$$

$$\frac{a}{2} M_A - b M_J - \frac{M_J}{1 + h_2 M_J} C = 0, \tag{3.24}$$

$$e = K. \tag{3.25}$$

Thus, the interior equilibrium is given by

$$C^* = \frac{1}{2} \frac{a e_2 \sqrt{\frac{bd_1}{(e_2 - d_1 h_2)\delta_1}}}{d_1} - \frac{e_2 b}{e_2 - d_1 h_2}, \tag{3.26}$$

$$M_A^* = \sqrt{\frac{bd_1}{(e_2 - d_1 h_2)\delta_1}}, \tag{3.27}$$

$$M_J^* = \frac{d_1}{e_2 - d_1 h_2}, \tag{3.28}$$

$$e^* = K. \tag{3.29}$$

Note that $M_A^* > 0$ and $M_J^* > 0$ if $e_2 - d_1 h_2 > 0$. $C^* > 0$ if $e_2 - d_1 h_2 > \frac{4bd_1\delta_1}{a^2}$. Therefore, the feasibility criteria for this system are

$$e_2 - d_1 h_2 > \frac{4bd_1\delta_1}{a^2}. \tag{3.30}$$

We next state the following theorem.

Theorem 3.3. *Consider the crab–mussel system* (2.1)–(2.4)*, there exists an interior steady state* (C^*, M_A^*, M_J^*, K) *when the epibiont reaches the equilibrium, that is* $e = K$*. And it is locally asymptotically stable under the following criteria*:

$$\frac{4bd_1\delta_1}{a^2} < e_2 - d_1 h_2 < \frac{16bd_1\delta_1}{a^2}, \quad d_1 > \frac{e_1}{h_1}. \tag{3.31}$$

The proof relies on the Routh–Hurwitz criterion,[31] and is relegated to Appendix Sec. A.3.

Remark 3. Note that the condition $d_1 > \frac{e_1}{h_1}$ is not a result of the Routh–Hurwitz criterion, rather it follows from Lemma A.1 in Appendix Sec. A.1. In a sense, we enforce it so that the attack rates should be as predicted via classical OFT.

3.4. *Global stability*

We now derive some results on the global stability of the internal equilibrium when $e = 0$.

Theorem 3.4. *Consider the models* (3.14)–(3.16)*. There exists an* $\epsilon > 0$*, s.t. the internal equilbrium point,* (C^*, M_A^*, M_J^*)*, is globally asymptotically stable under the following parametric restriction*:

$$\frac{d_1\delta_1}{a} < e_1 - d_1 h_1 < \frac{d_1}{\epsilon}, \quad 0 < \epsilon < \frac{a}{\delta_1}, \quad \frac{1}{2} < e_1 < 1. \tag{3.32}$$

Proof. Consider $M_A = \overline{M_A} + \epsilon$, under this transformation, we have the following transformed system:

$$\frac{dC}{dt} = -d_1 C + e_1 \frac{\overline{M_A} + \epsilon}{1 + h_1(\overline{M_A} + \epsilon)} C, \tag{3.33}$$

$$\frac{d\overline{M_A}}{dt} = bM_J - \delta_1(\overline{M_A} + \epsilon)^2 - \frac{\overline{M_A} + \epsilon}{1 + h_1(\overline{M_A} + \epsilon)} C, \tag{3.34}$$

$$\frac{dM_J}{dt} = a(\overline{M_A} + \epsilon) - bM_J. \tag{3.35}$$

It is enough to show the new system (3.33)–(3.35) is globally asymptotically stable. The equilibrium of (3.33)–(3.35) is given by

$$\begin{aligned} C^* &= \frac{e_1 a}{d_1}(\overline{M_A}^* + \epsilon) - \frac{e_1\delta_1}{d_1}(\overline{M_A}^* + \epsilon)^2, \\ \overline{M_A}^* &= \frac{d_1}{e_1 - d_1 h_1} - \epsilon, \\ M_J^* &= \frac{a d_1}{b(e_1 - d_1 h_1)}. \end{aligned} \tag{3.36}$$

Note that solutions to this new system are feasible if

$$\frac{d_1\delta_1}{a} < e_1 - d_1 h_1 < \frac{d_1}{\epsilon}, \quad 0 < \epsilon < \frac{a}{\delta_1}. \tag{3.37}$$

We define the following Lyapunov function:

$$V(C, \overline{M_A^*}, M_J) = C + \overline{M_A^*} + M_J. \tag{3.38}$$

Note that $V \geq 0$ because of the positivity of the solutions. Furthermore, V is radially unbounded. Now consider

$$\begin{aligned} \frac{dV}{dt} &= \frac{dC}{dt} + \frac{d\overline{M_A}}{dt} + \frac{dM_J}{dt} \\ &= -d_1 C + (e_1 - 1)\frac{\overline{M_A} + \epsilon}{1 + h_1(\overline{M_A} + \epsilon)} C - \delta_1(\overline{M_A} + \epsilon)^2 + a(\overline{M_A} + \epsilon), \\ &< -d_1 C - \delta_1(\overline{M_A} + \epsilon)^2 + a(\overline{M_A} + \epsilon) \\ &= -d_1 C - \delta_1(\overline{M_A})^2 - 2\delta_1\epsilon\overline{M_A} - \delta_1\epsilon^2 + a\overline{M_A} + a\epsilon \\ &= -d_1 C - \delta_1\left(\overline{M_A} - \frac{a}{2\delta_1}\right)^2 - \delta_1\left(\epsilon - \frac{a}{2\delta_1}\right)^2 + \frac{a^2}{2\delta_1} - 2\delta_1\epsilon\overline{M_A} \\ &= -\delta_1\left[\left(\overline{M_A} - \frac{a}{2\delta_1}\right)^2 + \left(\epsilon - \frac{a}{2\delta_1}\right)^2\right] + \frac{a^2}{2\delta_1} - 2\delta_1\epsilon\overline{M_A} - d_1 C. \end{aligned} \tag{3.39}$$

We hope $\frac{a^2}{2\delta_1} < \delta_1[(\overline{M_A} - \frac{a}{2\delta_1})^2 + (\epsilon - \frac{a}{2\delta_1})^2] + 2\delta_1\epsilon\overline{M_A} + d_1 C$. Since $2[(\overline{M_A} - \frac{a}{2\delta_1})^2 + (\epsilon - \frac{a}{2\delta_1})^2] \geq (\overline{M_A} - \epsilon)^2$, it is enough to show

$$\begin{aligned} \Rightarrow \frac{a^2}{\delta_1^2} &< (\overline{M_A} - \epsilon)^2 + 2\epsilon\overline{M_A} + \frac{2d_1 C}{\delta_1} \\ &= (\overline{M_A})^2 + \epsilon^2 + \frac{2d_1 C}{\delta_1}. \end{aligned} \tag{3.40}$$

Since $\overline{M_A}$ is bounded by $\frac{a}{\delta_1} - \epsilon$ from the feasibility conditions, we show

$$\Rightarrow \frac{a^2}{\delta_1^2} - \epsilon^2 < \left(\frac{a}{\delta_1} - \epsilon\right)^2 + \frac{2d_1 C}{\delta_1}, \tag{3.41}$$

$$\Rightarrow \frac{a}{\delta_1} < \epsilon + \frac{d_1 C}{\epsilon\delta_1}. \tag{3.42}$$

Since $\epsilon+\frac{d_1C}{\epsilon\delta_1} \geq 2\sqrt{\frac{d_1C}{\delta_1}}$, it is enough to show $\frac{a}{\delta_1} < 2\sqrt{\frac{d_1C}{\delta_1}}$. Due to $C^* = \frac{e_1a}{d_1}(\overline{M_A}^* + \epsilon) - \frac{e_1\delta_1}{d_1}(\overline{M_A}^* + \epsilon)^2 = \frac{e_1a}{d_1}M_A^* - \frac{e_1\delta_1}{d_1}(M_A^*)^2$, it is enough to show

$$\frac{a^2}{\delta_1} < 4d_1C = 4e_1aM_A - 4e_1\delta_1M_A^2$$

$$= -4e_1\delta_1\left(M_A - \frac{a}{2\delta_1}\right)^2 + \frac{2e_1a^2}{\delta_1}. \tag{3.43}$$

Therefore, we only need to show

$$\frac{a^2}{\delta_1} < \max\left(-4e_1\delta_1\left(M_A - \frac{a}{2\delta_1}\right)^2 + \frac{2e_1a^2}{\delta_1}\right) = \frac{2e_1a^2}{\delta_1}, \tag{3.44}$$

and this requires we have $\frac{1}{2} < e_1 < 1$.Then the system (3.14)–(3.16) is globally stable if

$$\frac{d_1\delta_1}{a} < e_1 - d_1h_1 < \frac{d_1}{\epsilon}, \quad 0 < \epsilon < \frac{a}{\delta_1}, \quad \frac{1}{2} < e_1 < 1. \tag{3.45}$$

□

Figure 2 gives an example on the global stability of this model.

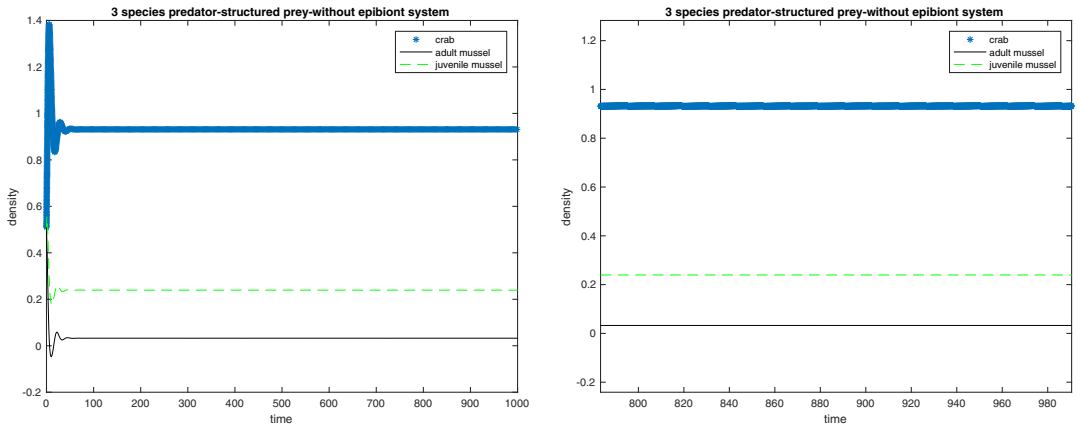

(a) (b)

Fig. 2. The above figures verify Theorem 3.4. We consider the parameters $e_1 = 0.9, e_2 = 0.01, d_1 = 0.2, b = 1, h_1 = 0.2, h_2 = 0.1, \delta_1 = 0.6, a = 0.8, \epsilon = 0.2$. (a) The initial condition $(C_0, M_{A0}, M_{J0}) = (0.5, 0.5, 0.5)$. (b) The initial condition $(C_0, M_{A0}, M_{J0}) = (500, 500, 500)$ (zooming in time scale). They both reach a stable level (0.9312, 0.0326, 0.2394).

Remark 4. Note, although we prove global stability (under certain parametric restrictions) for the case without epibiont ($e = 0$), it is easily proven using the same approach as above for the ($e = K$) case by just replacing $M_A = \overline{M_A} + \epsilon$ and defining a new Lyapunov function as $V(C, \overline{M_A}, M_J, e) = C + \overline{M_A} + M_J + e$.

4. Hopf Bifurcation

Now, we will investigate the Hopf bifurcation for the system in terms of parameter a. In this paper, we will follow the method developed by Liu.[32] First, let us consider the system (2.1)–(2.4), without the presence of an epibiont ($e = 0$), that is when $e = 0$. The Hopf bifurcation at $a = a_*$ can occur if $A_2(a_*), A_0(a_*)$, and $\phi(a_*) = A_2(a_*)A_1(a_*) - A_0(a_*)$ are smooth functions of a in an open interval of $a_* \in \mathbf{R}$ such that

(1) $A_1(a_*) > 0, A_0(a_*) > 0$, and $\phi(a_*) = A_2(a_*)A_1(a_*) - A_0(a_*) = 0$.
(2) $\frac{d\phi(a)}{da}|_{a=a_*} \neq 0$.

We check the above, in Sec. A.4, to state the following theorem.

Theorem 4.1. *Under the condition* (3.20), *there is a simple Hopf bifurcation of the positive equilibrium point* (C^*, M_A^*, M_J^*) *of model system* (3.14)–(3.16) *at some critical value of parameter* a_* *given by* (A.41) *and* (A.42).

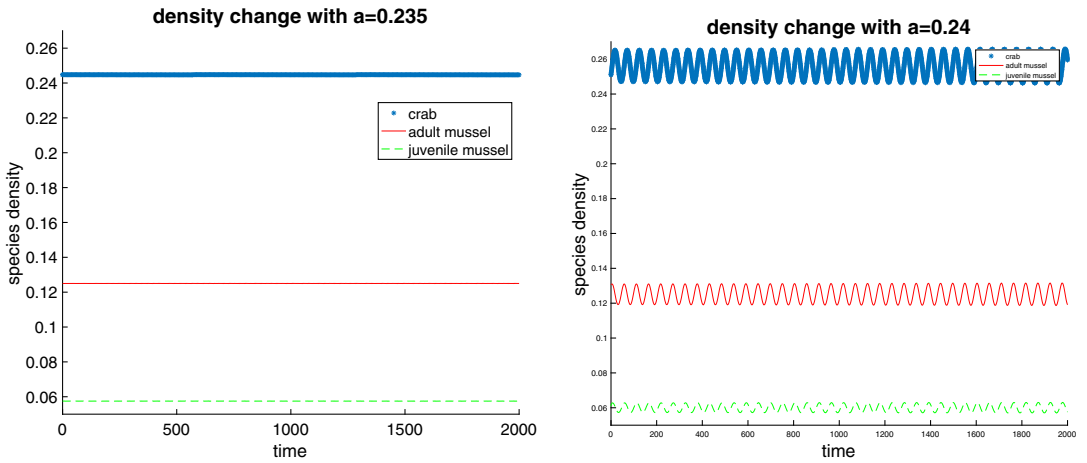

(a) (b)

Fig. 3. Here we demonstrate the species density change with time. We see in (a), the population of the species are stable when $a = 0.235$, while in (b) occurence of a Hopf bifurcation has lead to population cycles.

5. Optimal Control

In this section, our goal is to investigate mechanisms in our crab–mussel–epibiont system, that, if controlled, could lead to optimal levels of crab or mussel densities. We assume that the attack rates u_1 and u_2 are not known *a priori* and enter the system as time-dependent controls. They no longer depend on the epibiont density. Instead, we assume that the handling time depends on the epibiont density e in the following way:

where

$$h_1(e) = 1 + \frac{e}{K}, \quad a(e) = a\left(\frac{K - \frac{e}{2}}{K}\right). \tag{5.1}$$

These responses are for the range $0 \leq e \leq K$. Increase in epibiont density still negatively effects mussel fecundity and the handling time for adult mussels increases with increasing epibiont density.

This has a twofold advantage. We can visualize the system from the crab's point of view. That is, the crab can "optimally" control its attack rate, to reach the best possible population density. Also we can visualize the system from the mussel's point of view. That is, the mussel can induce defenses or other mechanisms, that would alter the attack rate of the crab, thus enabling the mussel population density to reach optimum levels. Our model takes the following form:

$$\begin{aligned} C' = &-d_1 C + e_1 u_1(t) \frac{M_A}{1 + h_1(e) u_1(t) M_A + h_2 u_2(t) M_J} C \\ &+ e_2 u_2(t) \frac{M_J}{1 + h_1(e) u_1(t) M_A + h_2 u_2(t) M_J} C, \end{aligned} \tag{5.2}$$

$$M_A' = bM_J - \delta_1 M_A^2 - u_1(t) \frac{M_A}{1 + h_1(e) u_1(t) M_A + h_2 u_2(t) M_J} C, \tag{5.3}$$

$$M_J' = a(e) M_A - bM_J - u_2(t) \frac{M_J}{1 + h_1(e) u_1(t) M_A + h_2 u_2(t) M_J} C, \tag{5.4}$$

$$e' = b_1 e \left(1 - \frac{e}{K}\right). \tag{5.5}$$

We next derive optimal strategies for three objective functions, where we maximize both crab and mussel populations. To simplify the calculation, we will consider the case when $e = K$, which is when the epibiont achieves carrying capacity. In this case, our system reduces to

$$\begin{aligned} C' = &-d_1 C + e_1 u_1(t) \frac{M_A}{1 + 2u_1(t) M_A + h_2 u_2(t) M_J} C \\ &+ e_2 u_2(t) \frac{M_J}{1 + 2u_1(t) M_A + h_2 u_2(t) M_J} C, \end{aligned} \tag{5.6}$$

$$M_A' = bM_J - \delta_1 M_A^2 - u_1(t) \frac{M_A}{1 + 2u_1(t) M_A + h_2 u_2(t) M_J} C, \tag{5.7}$$

$$M_J' = \frac{a}{2} M_A - bM_J - u_2(t) \frac{M_J}{1 + 2u_1(t) M_A + h_2 u_2(t) M_J} C. \tag{5.8}$$

5.1. *Maximizing crab denisty w.r.t. attacking rates*

To maximize density of the crab, the density of juvenile mussels (thus leading to more adult mussels, its favored food) should be maximized. Crab attack rates should

be miminized on the juvenile mussels, as they are less preferred by the crab. Thus, we choose the following objective functional:

$$J_1(u_1, u_2) = \int_0^T \left(C + M_J - \frac{1}{2}u_2^2\right)dt, \tag{5.9}$$

$$\text{s.t. } (5.6) - (5.8) \quad \text{and} \quad C(t_0) = C_0, \quad M_A(t_0) = M_{A_0}, \quad M_J(t_0) = M_{J_0}.$$

and we search for the optimal controls in the set U where

$$U = \{(u_1, u_2) \,|\, u_i \text{ measurable}, \ 0 \le u_1 \le 1, 0 \le u_2 \le 1, t \in [0, T], \forall\, T\}. \tag{5.10}$$

The goal is to seek an optimal (u_1^*, u_2^*) s.t.,

$$J_1(u_1^*, u_2^*) = \max_{(u_1,u_2)} \int_0^T \left(C + M_J - \frac{1}{2}u_2^2\right)dt. \tag{5.11}$$

We can state the following existence theorem.

Theorem 5.1. *Consider the optimal control problem* (5.6)–(5.8). *There exists* $(u_1^*, u_2^*) \in U$ *s.t.*

$$J_1(u_1^*, u_2^*) = \max_{(u_1,u_2)\in U} \int_0^T \left(C + M_J - \frac{1}{2}u_2^2\right)dt. \tag{5.12}$$

Proof. The compactness (closed and bounded in ODE case) of the functional J_1 follows from the global boundedness of the state variables via Theorem 3.3, and the boundedness assumption on the controls. Also the functional J_1 is concave in the argument u_2. This is easily verified via standard application.[33] These in conjunction give the existence of an optimal control via application of classical one predator–two prey theory.[34] □

In order to derive necessary conditions on the optimal control, we use Pontryagin's maximum principle (PMP). The Hamiltonian for our problem is given by

$$H = C + M_J - \frac{1}{2}u_2^2 + \lambda_1 C' + \lambda_2 M_A' + \lambda_3 M_J'. \tag{5.13}$$

We use the Hamiltonian to find a differential equation of the adjoint $\lambda_i, i = 1, 2, 3$.

$$\lambda_1'(t) = -\lambda_1 \left(-d_1 + \frac{M_A e_1 u_1 + M_J e_2 u_2}{M_A h_1 u_1 + M_J h_2 u_2 + 1}\right) + \frac{\lambda_2 u_1 M_A}{M_A h_1 u_1 + M_J h_2 u_2 + 1} + \frac{\lambda_3 u_2 M_J}{M_A h_1 u_1 + M_J h_2 u_2 + 1} - 1,$$

$$
\begin{aligned}
\lambda_2'(t) = &-\lambda_1\left(\frac{e_1u_1C}{M_Ah_1u_1+M_Jh_2u_2+1}-\frac{(M_Ae_1u_1+M_Je_2u_2)Ch_1u_1}{(M_Ah_1u_1+M_Jh_2u_2+1)^2}\right)\\
&-\lambda_2\left(-2\,\delta_1M_A-\frac{u_1C}{M_Ah_1u_1+M_Jh_2u_2+1}\right.\\
&\left.+\frac{{u_1}^2M_ACh_1}{(M_Ah_1u_1+M_Jh_2u_2+1)^2}\right)\\
&-\lambda_3\left(\frac{a}{2}+\frac{u_2M_JCh_1u_1}{(M_Ah_1u_1+M_Jh_2u_2+1)^2}\right),\\
\lambda_3'(t) = &-\lambda_1\left(\frac{e_2u_2C}{M_Ah_1u_1+M_Jh_2u_2+1}-\frac{(M_Ae_1u_1+M_Je_2u_2)Ch_2u_2}{(M_Ah_1u_1+M_Jh_2u_2+1)^2}\right)\\
&-\lambda_2\left(b+\frac{u_1M_ACh_2u_2}{(M_Ah_1u_1+M_Jh_2u_2+1)^2}\right)\\
&-\lambda_3\left(-b-\frac{u_2C}{M_Ah_1u_1+M_Jh_2u_2+1}+\frac{{u_2}^2M_JCh_2}{(M_Ah_1u_1+M_Jh_2u_2+1)^2}\right)-1,
\end{aligned}
\tag{5.14}
$$

with the transversality condition given as

$$
\lambda_1(T)=\lambda_2(T)=\lambda_3(T)=0. \tag{5.15}
$$

Considering the optimality conditions, the Hamiltonian function is differentiated with respect to control variables u_1 and u_2 resulting in

$$
\begin{aligned}
\frac{\partial H}{\partial u_1} =&\lambda_1\left(\frac{M_Ae_1C}{M_Ah_1u_1+M_Jh_2u_2+1}-\frac{(M_Ae_1u_1+M_Je_2u_2)CM_Ah_1}{(M_Ah_1u_1+M_Jh_2u_2+1)^2}\right)\\
&+\lambda_2\left(-\frac{M_AC}{M_Ah_1u_1+M_Jh_2u_2+1}+\frac{u_1{M_A}^2Ch_1}{(M_Ah_1u_1+M_Jh_2u_2+1)^2}\right)\\
&+\lambda_3\frac{u_2M_JCM_Ah_1}{(M_Ah_1u_1+M_Jh_2u_2+1)^2},\\
\frac{\partial H}{\partial u_2} =&\lambda_1\left(\frac{M_Je_2C}{h_1u_1M_A+h_2u_2M_J+1}-\frac{(e_1u_1M_A+e_2u_2M_J)CM_Jh_2}{(h_1u_1M_A+h_2u_2M_J+1)^2}\right)\\
&+\lambda_2\frac{u_1M_ACM_Jh_2}{(h_1u_1M_A+h_2u_2M_J+1)^2}\\
&+\lambda_3\left(-\frac{M_JC}{h_1u_1M_A+h_2u_2M_J+1}+\frac{u_2{M_J}^2Ch_2}{(h_1u_1M_A+h_2u_2M_J+1)^2}\right)-u_2.
\end{aligned}
\tag{5.16}
$$

We find a characterization of u_1^* by considering three cases:

$$\begin{aligned}
&\frac{\partial H}{\partial u_1} < 0 \Rightarrow u_1^* = 0,\\
&\frac{\partial H}{\partial u_1} = 0 \Rightarrow u_1^* = u_{1_1} \quad \text{s.t.} \quad \left.\frac{\partial H}{\partial u_1}\right|_{u_{1_1}} = 0,\\
&\frac{\partial H}{\partial u_1} > 0 \Rightarrow u_1^* = 1.
\end{aligned} \tag{5.17}$$

When the control is at the upper bound, u_{1_1} is strictly greater than 1. When the control is at the lower bound, the solution of u_{1_1} is strictly less than 0. Similarly for u_2^*. Thus a compact way of writing the optimal control is

$$\begin{aligned}
u_1^* &= \min(1, \max(0, u_{1_1})),\\
u_2^* &= \min(1, \max(0, u_{2_1})),
\end{aligned} \tag{5.18}$$

where u_{1_1} and u_{2_1} are given by

$$\begin{aligned}
u_{1_1} &= \frac{w_1}{w_2},\\
u_{2_1} &= \frac{-e_1\lambda_1 + \lambda_2}{M_J(e_1h_2\lambda_1 - e_2h_1\lambda_1 + h_1\lambda_3 - h_2\lambda_2)}.
\end{aligned} \tag{5.19}$$

with

$$\begin{aligned}
w_1 = \quad & CM_J{}^2e_1{}^3h_2{}^3\lambda_1{}^3 - 3\,CM_J{}^2e_1{}^2e_2h_1h_2{}^2\lambda_1{}^3 + 3\,CM_J{}^2e_1e_2{}^2h_1{}^2h_2\lambda_1{}^3\\
& -CM_J{}^2e_2{}^3h_1{}^3\lambda_1{}^3 + 3\,CM_J{}^2e_1{}^2h_1h_2{}^2\lambda_1{}^2\lambda_3 - 3\,CM_J{}^2e_1{}^2h_2{}^3\lambda_1{}^2\lambda_2\\
& -6\,CM_J{}^2e_1e_2h_1{}^2h_2\lambda_1{}^2\lambda_3 + 6\,CM_J{}^2e_1e_2h_1h_2{}^2\lambda_1{}^2\lambda_2 + 3\,CM_J{}^2e_2{}^2h_1{}^3\lambda_1{}^2\lambda_3\\
& -3\,CM_J{}^2e_2{}^2h_1{}^2h_2\lambda_1{}^2\lambda_2 + 3\,CM_J{}^2e_1h_1{}^2h_2\lambda_1\lambda_3{}^2 - 6\,CM_J{}^2e_1h_1h_2{}^2\lambda_1\lambda_2\lambda_3\\
& +3\,CM_J{}^2e_1h_2{}^3\lambda_1\lambda_2{}^2 - 3\,CM_J{}^2e_2h_1{}^3\lambda_1\lambda_3{}^2 + 6\,CM_J{}^2e_2h_1{}^2h_2\lambda_1\lambda_2\lambda_3\\
& -3\,CM_J{}^2e_2h_1h_2{}^2\lambda_1\lambda_2{}^2 + CM_J{}^2h_1{}^3\lambda_3{}^3 - 3\,CM_J{}^2h_1{}^2h_2\lambda_2\lambda_3{}^2\\
& +3\,CM_J{}^2h_1h_2{}^2\lambda_2{}^2\lambda_3 - CM_J{}^2h_2{}^3\lambda_2{}^3 + e_1e_2h_1{}^2\lambda_1{}^2 - e_1h_1{}^2\lambda_1\lambda_3\\
& -e_2h_1{}^2\lambda_1\lambda_2 + h_1{}^2\lambda_2\lambda_3,\\
w_2 = \quad & M_Ah_1{}^2(e_1{}^2h_2\lambda_1{}^2 - e_1e_2h_1\lambda_1{}^2 + e_1h_1\lambda_1\lambda_3 - 2\,e_1h_2\lambda_1\lambda_2 + e_2h_1\lambda_1\lambda_2\\
& -h_1\lambda_2\lambda_3 + h_2\lambda_2{}^2).
\end{aligned} \tag{5.20}$$

We can thus state the following theorem.

Theorem 5.2. *An optimal control* $(u_1^*, u_2^*) \in U$ *for the system* (5.6)–(5.8) *that maximises the objective functional* J_1 *is characterized by* (5.18).

5.2. *Maximizing mussel density w.r.t. attacking rates*

To maximinize mussel density, the attack rate on the adult mussels should be mini mized. We choose the following objective function:

$$J_2(u_1, u_2) = \int_0^T \left(M_A + M_J - \frac{1}{2}u_1^2 \right) dt, \tag{5.21}$$

$$\text{s.t. } (5.6) - -(5.8) \quad \text{and} \quad C(t_0) = C_0, \quad M_A(t_0) = M_{A_0}, \quad M_J(t_0) = M_{J_0}.$$

and we search for the optimal controls in the set U where

$$U = \{(u_1, u_2) \,|\, u_i \text{ measurable}, \ 0 \le u_1 \le 1, 0 \le u_2 \le 1, \ t \in [0, T], \ \forall T\}. \tag{5.22}$$

We can state the following existence theorem.

Theorem 5.3. *Consider the optimal control problem* (5.6)–(5.8). *There exists* $(u_1^*, u_2^*) \in U$ *s.t.*

$$J_2(u_1^*, u_2^*) = \max_{(u_1, u_2) \in U} \int_0^T \left(M_A + M_J - \frac{1}{2}u_1^2 \right) dt. \tag{5.23}$$

The proof is similar to Theorem 5.1.

Theorem 5.4. *An optimal control* $(u_1^*, u_2^*) \in U$ *for the system* (5.6)–(5.8) *that maximizes the objective function* J_2 *is characterized by*

$$\begin{aligned} u_1^* &= \min(1, \max(0, u_{1_2})), \\ u_2^* &= \min(1, \max(0, u_{2_2})). \end{aligned} \tag{5.24}$$

For details of the proof of the above necessary conditions and forms of u_{1_2}, u_{2_2} the reader is refered to Appendix in Sec. A.5.

5.3. *Maximizing mussel density w.r.t. intraspecific competition rate*

In this approach, we view the competition coefficient as a control. To reach certain optimal population densities, the mussels would maximize the densities of both adult and juvenile groups whilst minimising intraspecific competition. To this end, our system reduces to

$$C' = -d_1 C + e_1 u_1 \frac{M_A}{1 + 2u_1(t) M_A + h_2 u_2(t) M_J} C + e_2 u_2 \frac{M_J}{1 + 2u_1 M_A + h_2 u_2 M_J} C, \tag{5.25}$$

$$M_A' = bM_J - \delta_1(t) M_A^2 - u_1 \frac{M_A}{1 + 2u_1 M_A + h_2 u_2 M_J} C, \tag{5.26}$$

$$M_J' = \frac{a}{2} M_A - bM_J - u_2 \frac{M_J}{1 + 2u_1 M_A + h_2 u_2 M_J} C. \tag{5.27}$$

We choose the following objective function:

$$J_3(\delta_1) = \int_0^T \left(M_A + M_J - \frac{1}{2}\delta_1^2 \right) dt, \tag{5.28}$$

$$\text{s.t. } (5.25) - (5.27) \quad \text{and} \quad C(t_0) = C_0, \quad M_A(t_0) = M_{A_0}, \quad M_J(t_0) = M_{J_0}.$$

and we search for the optimal controls in the set U_1, where

$$U_1 = \{\delta_1 | \delta_1 \text{measurable}, \ 0 \leq \delta_1 \leq \infty, \ t \in [0, T], \ \forall T\}. \tag{5.29}$$

We can state the following existence theorem.

Theorem 5.5. *Consider the optimal control problem* (5.25)–(5.27). *There exist* $(u_1^*, u_2^*) \in U$ *s.t.*

$$J_3(\delta_1) = \max_{(u_1, u_2) \in U} \int_0^T \left(M_A + M_J - \frac{1}{2}\delta_1^2 \right) dt. \tag{5.30}$$

The proof is similar to Theorem 5.1.

Theorem 5.6. *An optimal control* $(u_1^*, u_2^*) \in U$ *for the system* (5.25)–(5.27) *that maximises the objective function* J_3 *is characterized by*

$$\delta_1^* = \max(0, -M_A^2 \lambda_2). \tag{5.31}$$

For the details of the proof of the above necessary conditions and forms of u_{1_2}, u_{2_2}, the reader is refered to the Appendix in Sec. A.6.

5.4. *Numerical simulations*

In this section, we investigate via numerical simulation and compare the species' population of the control system (5.2)–(5.5) and the classical system (2.1)–(2.4) under the epibiont achieving the carrying capacity ($e = K$). The solutions of the state and adjoint equations are *a priori* bounded. This follows via Theorem 3.1. Also, note that the Objective functions (see Secs. 5.1–5.3), are concave in the control variables. Thus, the optimal controls exist by using classical results from Fleming and Rishel [Chapter III, Theorem 2.1, p. 63].[34] Our goal is to now apply this theory to compute various optimal scenarios. To this end, we use a Forward–Backward Sweep iteration algorithm, and perform various numerical simulations. The parameter set chosen for our simulation is given in (5.32). The unit of time is days. We choose parameters in accordance with the biological literature, so our simulations are realistic. A more thorough discussion of how this is done is presented in the discussion section.

$$\begin{aligned} &d_1 = 0.015, \quad e_1 = 0.9, \quad e_2 = 0.5, \quad h_1 = 2.0, \quad h_2 = 1.0, \quad b = 0.05, \\ &\delta_1 = 0.1, \quad a = 0.3, \quad C(0) = 1, \quad M_A(0) = 1, \quad M_J(0) = 1. \end{aligned} \tag{5.32}$$

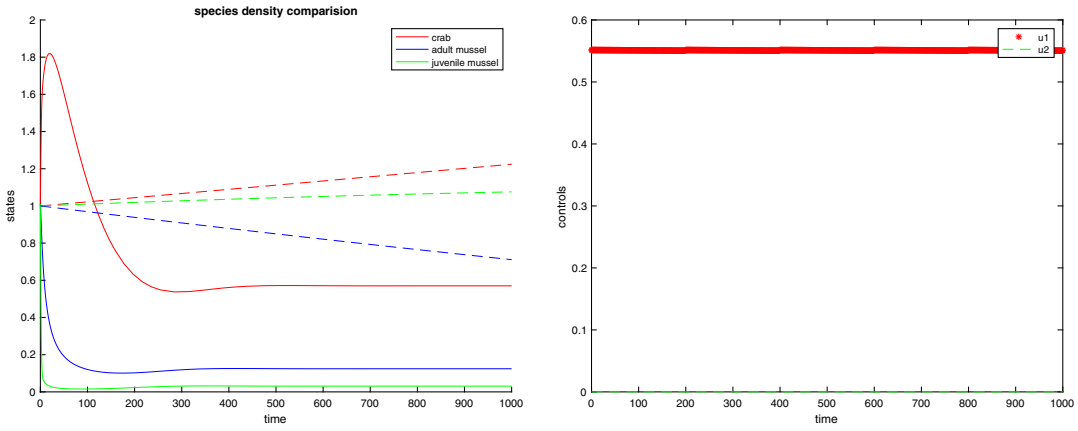

(a) (b)

Fig. 4. (a) Solid curves are the density change for each species of the system (2.1)–(2.4) with $e = K$ and the dashed line are the optimal state of the control system (5.2)–(5.5) for the objective function $J_1(u_1, u_2)$. (b) Optimal controls of $J_1(u_1, u_2)$ with the above parameter set (5.32).

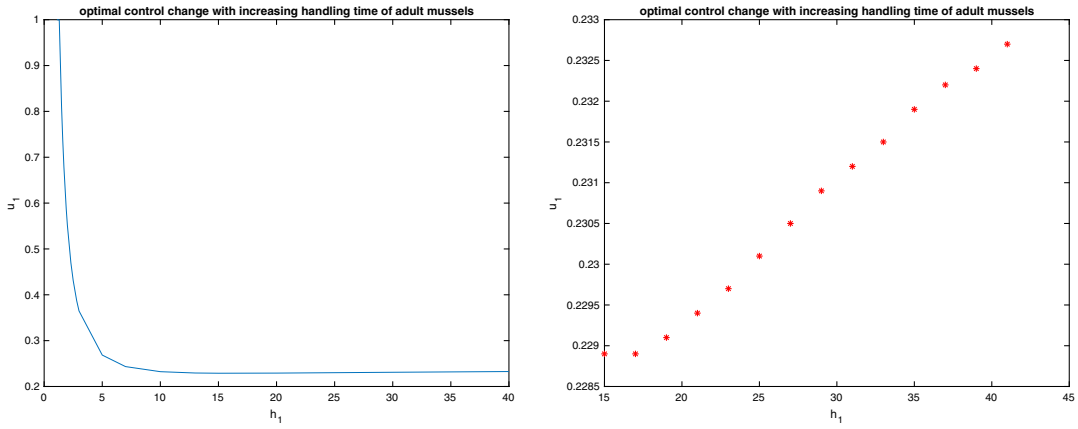

(a) (b)

Fig. 5. (a) Optimal control u_1 changes with increasing h_1 and (b) u_1 increases slightly with large h_1.

In Fig. 5, we set $h_1 = 2$ since $h_1 = 1 + \frac{e}{K}$, however, if we just assume h_1 as a constant and increase h_1 and keep other parameters the same, we found the optimal control u_2 always to be 0, and u_1 decreases and gradually become stable. In fact, when h_1 achieves to some critical value, u_1 begins to increase slightly.

The optimal foraging strategies are $u_1 = 0$ and $u_2 = 1$ for the system (2.1)–(2.4) under $e = K$. However, for the control system (5.2)–(5.5), $J_1(u_1, u_2)$ will be maximized when $u_1 = 0.5515$, $u_2 = 0$; $J_2(u_1, u_2)$ will be maximized when $u_1 = 0$, $u_2 = 0.9937$ and $J_3(\delta_1)$ will be maximized when $\delta_1 = 0$ with parameters in (5.32) which are shown in Figs. 4–8. Therefore, the optimal control approach does increase the targeted population.

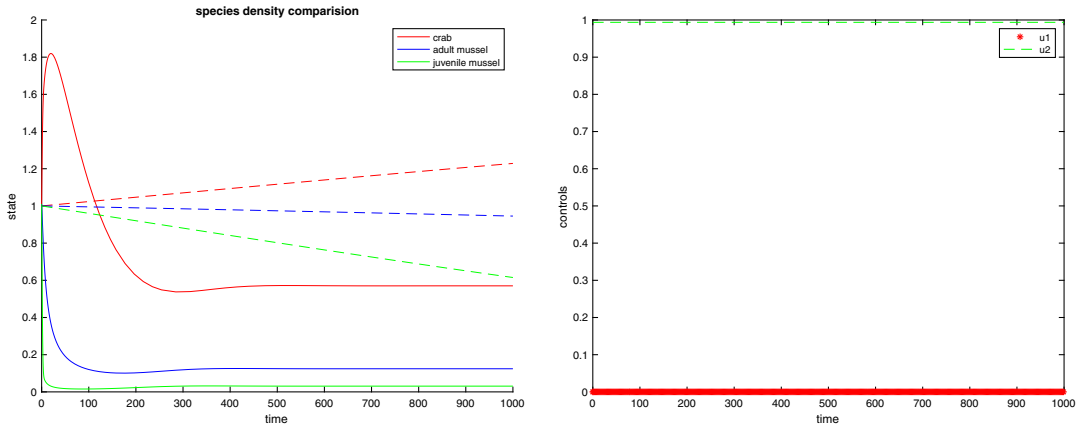

(a) (b)

Fig. 6. (a) Solid curves are the density change for each species of the system (2.1)–(2.4) with $e = K$ and the dashed line are the optimal state of the control system (5.2)–(5.5) for the objective function $J_2(u_1, u_2)$. (b) Optimal controls for $J_2(u_1, u_2)$ with the above parameter set shown in (5.32).

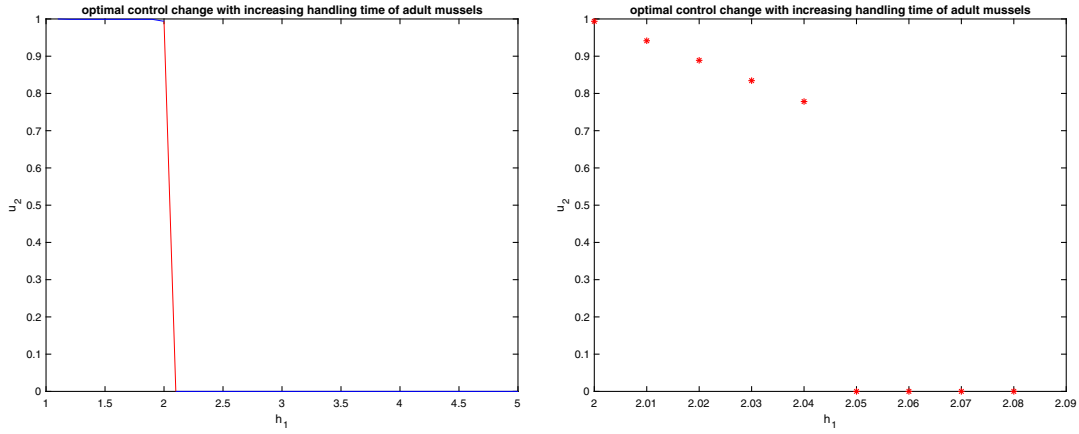

(a) (b)

Fig. 7. In this simulation, we look at how u_2 changes w.r.t. h_1. Here $h_2 = 1$. We want to see the change of the control u_2 as h_1 increases. The control $u_1 = 0$ no matter how large h_1 is. What we notice is that u_2 suddenly goes down to 0 from 0.7783, at a critical value $h_1^* = 2.05$.

Remark 5. Based on the initial condition $(C(0), M_A(0), M_J(0)) = (1, 1, 1)$, we see that the juvenile mussel population size dropped over 90% (1–0.03) of the dynamics (2.1)–(2.4) with $e = K$ in a few days in Figs. 4–8. Note, this is solely a feature of the chosen parameters and initial conditions (that is for these parameters the steady states are fairly low, ≈ 0.03). Thus, given the chosen parameters, the dynamics causes a decay to the juvenile mussel steady state fairly quick. In Figs. 9–10, we see as we vary parameters and initial conditions, this can change to predict a more realistic ecological scenario.

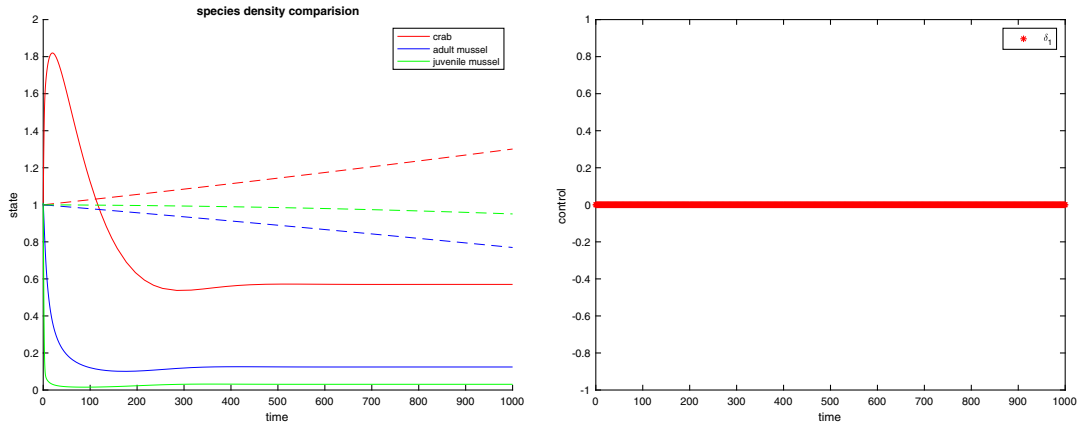

(a) (b)

Fig. 8. (a) Solid curves are the density change for each species of the system (2.1)–(2.4) with $e = K$ and the dashed line are the optimal state of the control system (5.2)–(5.5) for the objective function $J_3(\delta_1)$. (b) The optimal control for the objective function J_3 is always to be $\delta_1 = 0$.

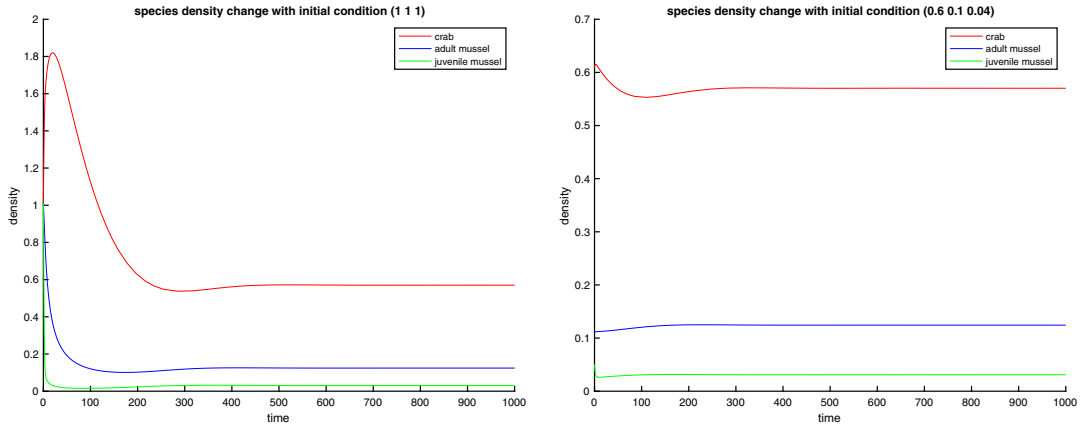

(a) (b)

Fig. 9. Here we simulate the dynamics of our system (2.1)–(2.4) (in the case of $e = K$) with same parameters but different initial conditions. We take $d_1 = 0.015, e_1 = 0.9, e_2 = 0.5, h_1 = 2, h_2 = 1$, $b = 0.05, \delta_1 = 0.1$ and $a = 0.3$. (a) The initial condition is $(1, 1, 1)$. (b) The initial condition is $(0.6, 0.1, 0.04)$. Both initial conditions go to same steady state $(0.5722, 0.1244, 0.0309)$ but with different decay rates. Also, it is seen in (b), that it takes about 200 days for the populations to reach steady levels. Therein, the mussel populations actually rise, and the fall in the crab population is not to drastic.

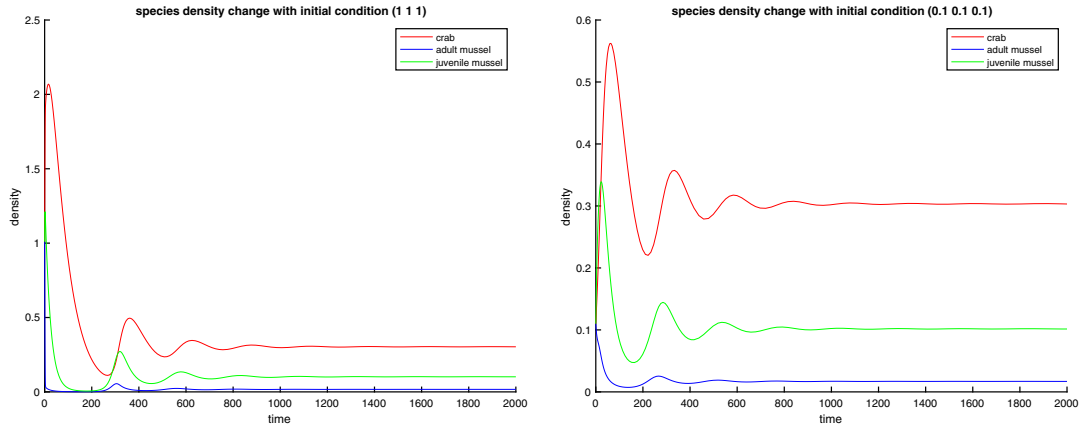

(a) (b)

Fig. 10. Here we simulate the dynamics of our system (2.1)–(2.4) (in the case of $e = 0$) with different initial conditions. We take $d_1 = 0.015, e_1 = 0.9, e_2 = 0.5, h_1 = 1, h_2 = 0.2, b = 0.05, \delta_1 = 0.1$ and $a = 0.3$. (a) The initial condition is $(1, 1, 1)$. (b) The initial condition is $(0.1, 0.1, 0.1)$. Both initial conditions go to same steady state $(0.3020, 0.171, 0.01023)$ but with different decay rates. Herein, we choose $h_2 = 0.2$, to model a case where the handling times of juvenile mussel is five times less than that of handling an adult mussel.

6. Discussion and Conclusion

Epibiotic invasive species often have anti-predator defenses that are behavioral, chemical, or mechanical,[35,36] giving them a survival advantage in a novel habitat because potential predators avoid using them as a food source.[37,38] While this provides a benefit to the basibiont, it impacts other members of the community, including predators of the basibiont as they may show lower preference for basibionts that are overgrown by invasive epibionts.[10,39] However, the effects of epibionts on basibionts are not always positive. Many times the epibiont may attract predators resulting in consumption of the epibiont, which automatically leads to consumption of the basibiont. This is referred to in the literature as "shared doom".[18] Epibionts can also negatively affect basibiont fecundity and fitness, resulting in fewer offspring.[9] In essence, invasion of predator–prey communities by epibionts is complex, and warrants a thorough mathematical investigation of their impact on predator–prey interactions and populations.

Population cycles are common in predator–prey communities, and although these are possible in our model without epibionts, extensive numerical simulations indicate that at carrying capacity $e = K$, a Hopf bifurcation is *not* possible. This points to the epibiont having a stabilizing influence in that it can eliminate population oscillations. A rigorous proof of this is an interesting future direction. Within our study, Theorem 3.4 tells us that if the energy gain from the adult mussel is in a certain critical region $0 < e_1 < 1$, then one has global stability; even very large perturbations would still allow the system to return to its base state.

Our central question focuses on the effect of the introduced epibiont on the population densities of the local crab–mussel communities. Could high epibiont density lead to lower mussel populations (and so subsequently lower crab populations)? To answer this, we compare the equilibrium levels of the juvenile mussel population in two cases, one in which there is no epibiont, and the other in which the epibiont reaches carrying capacity. If the epibionts do have an adverse effect, then we would have

$$M_J^*|_{(e=K)} < M_J^*|_{(e=0)}.$$

Comparing these yields

$$be_1 + d_1h_2a < ae_2 + d_1h_1b. \tag{6.1}$$

Although we know $e_1 > e_2$, under high epibiont density ($e = K$), we have $h_1 \gg h_2$, thus even if $a > b$, (6.1) could easily hold meaning that there is an adverse effect on the juvenile mussel density via epibiont presence, leading to fewer adults subsequently, and so epibionts could clearly be a factor in mussel population declines as seen via data from the Gulf of Maine.[8] Such decline could eventually lead to crab population decline as well, if the crab species is a specialist on mussels. However, the effects of epibionts on mussel fecundity could also be a cause of predator decline. In order to understand the effects of epibiosis, we investigate the equilibrium density of the crab populations for the "no epibiont" case versus the "carrying capacity" case. What we note is

$$C^*|_{(e=0)} = \frac{e_1(a(e_1 - d_1h_1) - d_1\delta_1)}{(e_1 - d_1h_1)^2}, \tag{6.2}$$

$$C^*|_{(e=K)} = \frac{1}{2}\frac{ae_2\sqrt{\frac{bd_1}{(e_2-d_1h_2)\delta_1}}}{d_1} - \frac{e_2b}{e_2 - d_1h_2}. \tag{6.3}$$

Clearly, as epibiont cover reduces mussel fecundity from a to $\frac{a}{2}$, this directly affects the crab population. In the $(e = K)$ case, there is an increase by a factor of only $\frac{a}{2}$, as opposed to a factor of a in the $(e = 0)$ case. Thus reduced fecundity in mussels due to epibiont cover, can also reduce crab populations as well.

We assume logistic growth in the epibiont density. Although in the Gulf of Maine epibiont density fluctuates seasonally, our model could be a useful predictive tool in periods where logistic growth is seen. In locations, such as Japan and New Zealand, the epibiont *D. vexillum* grows logistically[9] due to water temperatures staying above, the threshold for *D. vexillum* viability.

Note, we have used the biology literature in order to come up with realistic parameter values for our numerical simulations. *Carcinus maenas* crabs seem to vary in lifespan, ranging from 3–4 years on the west coast of the US in Oregon[40] to 6 years in Maine.[41] Klassen and Locke[42] summarized *C. maenas* life span to be between 4–7 years in their biological synopsis of the species. Note, *C. maenas* can survive up to three months without food. Thus, from Eq. (2.1), if there were no

mussels present, we should have the crabs survive up to 90–100 days. This yields the death rate of the crab, $d_1 \approx 0.015$.

Mussel life span varies greatly, depending on whether or not predators are present. For example, in subtidal areas when exposed to predators, mussels lived from 2 to 3 years.[44] At higher zones on the same shoreline, in the absence of predators, they reached 15–20 years of age. At a site in England, mussels rarely lived into their third year,[45] but in an extremely high latitude, they were found living from 18 to 24 years.[46] We model, based on the lower numbers as in our setting, the mussels that are exposed to predators (and those seem to be more typical numbers in the field). Mussels become sexually mature at about 1 year.[47,48] One study found mussels reaching maturity at just over 1 year.[43] The size at which mussels become mature has varied in reports since there are several factors that determine mussel growth; these sizes vary anywhere between 4 mm and 35 mm, though it seems that most mussels are somewhere between 20 mm and 30 mm in size.[48] However, our modeling scenario compartmentalizes mussels as adults or juveniles, based on when they lose their periostracum. Mussels lose their periostracum sometime between 3 mm and 5 mm in size,[49] when they become fouled by epibionts. Thus, there is some leeway we have in choosing the maturation rate b, of mussels from juveniles to adults, as there clearly is a size difference (thus a time lag) between when the they lose their periostracum (3–5 mm), to when they sexually mature (4–35 mm). Thus, we model the maturation rate b, to be in the range 0.005–0.01, that is maturing to loose their periostracum, in the range of 100–200/250 days — just short of their sexual maturity of 300 days–1 year. Detailed simulations via these parameters are provided in Sec. 5.4. Also, note the handling times h_1 and h_2, are to be understood in a relative sense. So, h_1 is the time it takes for crabs to handle adult mussels, and h_2 is the time it takes for crabs to handle juvenile mussels. Our premise is that, under high epibiont cover, it takes mussels twice as long to handle adults. Here, we refer to Ref. 10, which finds the handling time, could vary anywhere between staying roughly the same to maybe six times longer. An interpretation of $h_1 = 2$ and $h_2 = 1$, would mean it takes the crabs twice as long to handle the adult mussels, as it takes to handle juveniles. Detailed simulations to this end are also provided in Sec. 5.4.

We also use optimal control theory to visualize various optimal scenarios to maximize each crab and mussel densities. Herein, we change the problem slightly, and assume the attack rates u_1, u_2 are not known *a priori*, but are time-dependent. Our objective is to explore various scenarios that a species of crab or mussel might attempt to optimize, by manipulating the attack rates. Epibionts are assumed to be present, and their effect is modeled via increasing the handling time h_1 of adult mussels, as epibiont density increase.

Simulations suggest (Fig. 4(a)) that even under high epibiont density (which in this scenario amounts to doubled h_1), the crab should *not* attack juvenile mussels,

but attempt to attack adults. Figure 4(b) demonstrates, that what is optimal for the mussel is if $u_1 = 0$, and so the adult mussel must induce defenses to reduce u_1, even if it realistically cannot drive that rate to zero. This confirms experimental results of rapid shell thickening by mussels, seen via Ref. 12.

Figure 5(a) looks at the attack rate on adut mussels u_1, as h_1 changes. Here, we are trying to maximize mussel populations, and u_1 decreases as h_1 increases, as expected. However, u_1 is approximately 0.23; that is, it does not change significantly if handling times become very large. Curiously, it goes up ever so slightly as shown in Fig. 5(b). This likely corresponds to the adult mussel thickening its shell just enough to increase handling time by the crab.

Figure 7 looks at the attack rate on juvenile mussels u_2, as h_1 changes. Here again we are trying to maximize mussel populations. When handling time on adults is low, juvenile mussels are protected from crab predation due to the predators preference for larger mussels. However, when handling time on adults is high (greater than 2.05 in this simulation), it is likely that crabs would switch to the juvenile; therefore, juveniles must be able to disperse or seek refuge in order to bring attack rates on the juvenile mussels to zero (in turn maximizing their population size). Young mussels drift in the water column until they reach a size of approximately 2.5 mm, then they settle on a filamentous algal substrate.[3] Some mussel species settle on algal substrate until they are 30 mm in length.[50] This substrate acts as refuge and must be available for juveniles in order to maximize mussel populations. However, with degradation of suitable habitat, the opportunities for escape from crab populations becomes diminished. Major disturbance events, either natural or anthropogenic, in conjunction with invasion by substrate-smothering colonial species and voracious predators, are likely to decrease opportunities for escape. Endeavors to model predator–prey systems incorporating prey refuge may yield surprising results on stability.[51,52] Thus, it would be very interesting to model refuge effects for the juvenile mussels herein.

As a future direction in modeling the crab–mussel–epibiont interaction, we would also like to examine interference effects.[53–55] This effect has often seen to be stabilizing,[56] and thus modeling interference among the crab population, at high epibiont density is also realistic. Note, Theorem 5.6 suggests that eliminating intraspecific competition among mussels is optimal from their point of view, and yields a maximum density, if there was *no* competition present. Future modeling endeavors may also investigate if high epibiont cover promotes cannibalism in crabs. That is, under high epibiont cover of adult mussels, would a crab prefer to cannibalize its own conspecifics,[57,58] rather than switching to juvenile mussels? Another interesting future direction is to look at the foraging of crabs as they move in and out of patches containing mussels, some of which might be protected by mussel farmers, akin to marine protected areas.[59,60] A spatially explicit approach to this end, modeling a changing habitat based on mussel density, would also be interesting.[61]

The empirical literature shows that while epibionts alter the prey choice of predators, including crabs and sea stars,[17,21–23] there are no prey switching experiments using *D. vexillum*. Our goal is to provide firm modeling grounds for the scope of such experiments in the future. Thus a logical next step for empirical studies is to conduct experiments with *D. vexillum* to confirm our switching hypothesis, as well as look at switching scenarios under varying levels of overgrowth (with both living and artificial epibionts such as in Ref. 21). An interesting research question therein would be to ask if one sees the inverted parabola-shaped curve, typical of OFT scenarios when measuring crab size versus mussel preference. If our switching hypothesis is confirmed, this should not be the case, as smaller size juvenile mussels should be preferred to adults under heavy epibiont cover. All in all, we hope our results will help devise suitable strategies and measures that will enable a boost in dwindling mussel populations, particularly as new complexities arise in ecosystems, driven by rapid increase in invasions.

Acknowledgement

RP and JL would like to acknowledge partial support from the National Science Foundation via DMS 1715377 and DMS 1839993.

References

1. *Profile of the Blue Mussel* (*Mytilus edulis*) *Gulf Region. Policy and Economics Branch*, *Gulf Region*. Department of Fisheries and Oceans, Moncton, New Brunswick, February, 2003.
2. *Food and Aquaculture Organization of the United Nations* [*FAO*] *Cultured Aquatic Species Information Programme*. Mytilus edulis. In: FAO Fisheries and Aquaculture Department [online], http://www.fao.org/fishery/culturedspecies/Mytilus_edulis/en#tcNA00D6. Update 1 January 2004 [Accessed 28 June 2017].
3. Seed R, Suchanek TH, Population and community ecology of Mytilus, in Gosling, E [ed.], *The Mussel Mytilus*: *Ecology*, *Physiology*, *Genetics and Culture*. Developments in Aquaculture and Fisheries Science, Vol. 25, Elsevier, Amsterdam, pp. 87–169, 1992.
4. Menge BA, Components of predation intensity in the low zone of the New England rocky intertidal region, *Oecologia* (*in Berl.*) **58**:141–155, 1983.
5. Suchanek TH, Mussels and their role in structuring rocky shore communities, in Moore PG, Seed R (eds.), *The Ecology of Rocky Coasts. Hodder and Stoughton*, Sevenoaks, UK, pp. 70–96, 1985.
6. Widdows J, Donkin P, Mussels and environmental contaminants: Bioaccumulation and physiological aspects, in Gosling, E [ed.], *The Mussel Mytilus*: *Ecology*, *Physiology*, *Genetics and Culture. Developments in Aquaculture and Fisheries Science*, Vol. 25, Elsevier, Amsterdam, pp. 383–424, 1992.
7. Tsuchiya M, Nishihara M, Islands of Mytilus as a habitat for small intertidal animals: Effect of island size on community structure, *Marine Ecol Prog Ser* **25**:71–81, 1985.
8. Sorte CJB, Davidson VE, Franklin MC, Benes KM, Doellman MM, Etter RJ, Hannigan RE, Lubchenco J, Menge BA, Long-term declines in an intertidal foundation species parallel shifts in community composition, *Global Change Biol* **23**(1):341–352, 2017.

9. Auker L *et al.*, The effects of Didemnum vexillum overgrowth on Mytilus edulis biology and ecology, PhD thesis, University of New Hampshire, 2010.
10. Auker L *et al.*, Exploring biotic impacts from carcinus maenas predation and didemnum vexillum epibiosis on mytilus edilus in the gulf of maine, *Northeast Nat* **21**(3):479–494, 2014.
11. DeGraaf JD, Tyrrell MC, Comparison of the feeding rates of two introduced crab species, Carcinus maenas and Hemigrapsus sanguineus, on the Blue Mussel, Mytilus edulis, *Northeast Nat* **11**(2):163–167, 2004.
12. Freeman AS, Byers JE, Divergent induced responses to an invasive predator in marine mussel populations, *Science* **313**:831–833, 2006.
13. Elner RW, The mechanics of predation by the shore crab Carcinus maenas (L.) from Port Herbert, Southwestern Nova Scotia, *J Shellfish Res* **1**:89–94, 1978.
14. Jubb CA, Hughes RN, Ap Rheinallt T, Behavioral mechanisms of size-selection by crabs, Carcinus maenas (L.) feeding on mussels, Mytilus edulis L, *J Exp Marine Biol Ecol* **66**(1):81–87.
15. Frandsen R, Dolmer P, Effects of substrate type on growth and mortality of blue mussels (Mytilus edulis) exposed to the predator Carcinus maenas, *Marine Biol* **141**(2):253–262, 2002.
16. Dijkstra J, Harris LG, Westerman E, Distribution and long-term temporal patterns of four invasive colonial ascidians in the Gulf of Maine, *J Exp Marine Biol Ecol* **342**:61–68, 2007.
17. Bullard SG *et al.*, The colonial ascidian Didemnum sp. A: Current distribution, basic biology and potential threat to marine communities of the northeast and west coasts of North America, *J Exp Marine Biol Ecol* **342**:99–108, 2007.
18. Laudien J, Wahl M, Indirect effects of epibiosis on host mortality: Seastar predation on differently fouled mussels, *Marine Ecol* **20**:35–47, 1999.
19. Wahl M, Krger K, Lenz M, Non-toxic protection against epibiosis, *Biofouling* **12**:205–226, 1998.
20. Harper EM, Skelton PW, A defensive value of the thickened periostracum in the Mytiloidea, *Veliger* **36**(1):36–42, 1993.
21. Enderlein P, Moorthi S, Rohrscheidt H, Wahl M, Optimal foraging versus shared doom effects: Interactive influence of mussel size and epibiosis on predator preference, *J Exp Marine Biol Ecol* **292**:231–242, 2003.
22. Thornber C, Associational resistance mediates predator–prey interactions in a marine subtidal system, *Marine Ecol* **28**:480–486, 2007.
23. Valeria Bers A, D'Souza F, Klinjstra J, Willemsen P, Wahl M, Chemical defence in mussels: Antifouling effect of crude extracts of the periostracum of the blue mussel Mytilus edulis, *Biofouling* **22**(4):251–259, 2006.
24. Davies NB, Prey selection and the search strategy of the spotted flycatcher (Muscicapa striata): A field study on optimal foraging, *Animal Behav* **25**:1016–1033, 1977.
25. Krivan V, Optimal foraging and predator-prey dynamics, *Theor Popul Biol* **49**:265–290, 1996.
26. Krivan V, Sikder A, Optimal foraging and predator-prey dynamics II, *Theor Popul Biol* **55**:111–126, 1999.
27. Van Baalen M, Kivan V, van Rijn PC, Sabelis MW, Alternative food, switching predators, and the persistence of predator-prey systems, *Am Nat* **157**(5):512–524, 2001.
28. Werner EE, Mittelbach GG, Optimal foraging: Field tests of diet choice and habitat switching, *Am Zool* **21**(4):813–829, 1981.

29. Larsen PS, Riisgard HU, Growth-prediction model for blue mussels (Mytilus edulis) on future optimally thinned farm-ropes in Great Belt (Denmark), *J Marine Sci Eng* **4**, 2016.
30. Evans LC, *Partial Differential Equations*, American Mathematical Society, Providence, RI, 1993.
31. Perko L, *Differential Equations and Dynamical Systems*, Springer Science & Business Media, Vol. 7, 2013.
32. Liu WM, Criterion of hopf bifurcations without using eigenvalues, *J Math Anal Appl* **182**:250–256, 1994.
33. Lenhart S, Workman JT, *Optimal Control Applied to Biological Models*, Crc Press, 2007.
34. Fleming WH, Rishel RW, *Deterministic and Stochastic Optimal Control*, Springer Verlag, New York, 1975.
35. Chapman D, Ranelletti M, Kaushik S, Invasive marine algae: An ecological perspective, *Botan Rev* **72**(2):153–178, 2006.
36. Wolfe LM, Why alien invaders succeed: Support for the escape-from-enemy hypothesis, *Am Nat* **160**:705–711, 2002.
37. Callaway RM, Ridenour WM, Novel weapons: Invasive success and the evolution of increased competitive ability, *Front Ecol Environ* **2**:436–443, 2004.
38. Pisut DP, Pawlik JR, Anti-predatory chemical defenses of ascidians: Secondary metabolites or inorganic acids? *J Exp Marine Biol Ecol* **270**:203–214, 2002.
39. Wahl M, Hay ME, Associational resistance and shared doom: Effects of epibiosis on herbivory, *Oecologia* **102**:329–340, 1995.
40. Yamada SB, Kalin A, Hunt C, Growth and longevity of the European green crab Carcinus maenas, in the Pacific Northwest, *2nd Int Conf Bioinvasions*, 2001.
41. Berrill M, The life cycle of the green crab Carcinus maenas at the northern end of its range, *J Crustacean Biol* **2**(1):31–39, 1982.
42. Klassen GL, Locke A, A biological synopsis of the European green crab, Carcinus maenas, *Can Manuscr Rep Fish Aquat Sci.* 2818:vii.+75pp, 2007.
43. Sunila I, Reproduction of Mytilus edulis L. (Bivalvia) in a brackish water area, the Gulf of Finland, *Annls Zool Fenn* **18**:121–128, 1981.
44. Seed R, The ecology of Mytilus edulis L. (Lamellibranchiata) on exposed rocky shores. 2. Growth and mortality, *Oecologia* **3**:317–350, 1969.
45. Dare PJ, Settlement, growth, and production of the mussel Mytilus edulis L. in Morecambe Bay, *Fishery Invest* **28**:1–25, 1976.
46. Theisen BF, The growth of Mytilus edulis L. (Bivalvia) from Disko and Thule district, Greenland, *Ophelia* **12**:59–77, 1973.
47. Seed R, The ecology of Mytilus edulis L. (Lamellibranchiata) on exposed rocky shores. I. Breeding and settlement, *Oecologia* **3**:277–316, 1969.
48. Sprung M, Reproduction and fecundity of the mussel Mytilus edulis at Helgoland (North Sea), *Helgolnder Meeresuntersuchungen* **36**:243–255, 1983.
49. Wahl M, Krger K, Lenz M, Non-toxic protection against epibiosis, *Biofouling* **12**(1–3):205–226, 1998.
50. Moreno CA, Macroalgae as a refuge from predation for recruits of the mussel Choromytilus chorus (Molina, 1782) in Southern Chile, *J Exp Marine Biol Ecol* **191**(2):181–193, 1995.
51. Krivan V, Priyadarshi A, L-shaped prey isocline in the Gause predator-prey experiments with a prey refuge, *J Theor Biol* **370**:21–26, 2015.
52. Parshad RD, Qansah E, Black K, Beauregard M, Biological control via "ecological" damping: An approach that attenuates non-target effects, *Math Biosci* **273**:23–44, 2016.

53. Negi K, Gakkhar S, Dynamics in a BeddingtonDeAngelis preypredator system with impulsive harvesting, *Ecol Model* **206**(3–4):421–430, 2007.
54. Gupta K, Gakkhar S, The Filippov approach for predator-prey system involving mixed type of functional responses, *Differential Equations and Dynamical Systems* 1–21, 2016.
55. Parshad RD, Bhowmick S, Quansah E, Basheer A, Upadhyay RK, Predator interference effects on biological control: The paradox of the generalist predator revisited, *Commun Nonlinear Sci Numer Simul* **39**:169–184, 2016.
56. Pribylova L, Berec L, Predator interference and stability of predator-prey dynamics, *J Math Biol* **71**:301–323, 2015.
57. Basheer A, Quansah E, Bhowmick S, Parshad RD, Prey cannibalism alters the dynamics of Holling Tanner-type predator prey models, *Nonlinear Dyn* **85**(4):2549–2567, 2016.
58. Basheer A, Lyu J, Giffin A, Parshad RD, The destabilizing effect of cannibalism in a spatially explicit three-species Age structured predator-prey model, *Complexity* **2017**, 2017.
59. Jiao J, Pilyugin SS, Osenberg CW, Random movement of predators can eliminate trophic cascades in marine protected areas, *Ecosphere* **7**(8): 2016.
60. Pilyugin SS, Medlock J, De Leenheer P, The effectiveness of marine protected areas for predator and prey with varying mobility, *Theor Popul Biol* **110**:63–77, 2016.
61. Li B, Bewick S, Shang J, Fagan WF, Persistence and spread of a species with a shifting habitat edge, *SIAM J Appl Math* **74**(5):1397–1417, 2014.

Appendix A

A.1. *Optimal strategy in our setting*

Here, we give a rigorous reasoning for our switching hypothesis. If one considers classical optimal foraging theory (OFT), we can define a fitness function

$$R(u_1, u_2) = \frac{e_1 u_1 M_A}{1 + h_1 u_1 M_A + h_2 u_2 M_J} + \frac{e_1 u_1 M_J}{1 + h_1 u_1 M_A + h_2 u_2 M_J}. \tag{A.1}$$

We endeavor to maximize $R(u_1, u_2)$, the net rate of energy intake during foraging. The optimal strategy for a crab (according to classical OFT) relies on the density of mussels. That is for each (M_A, M_J), we get a set of optimal controls $S(M_A, M_J)$ known as the strategy map.

$$S(M_A, M_J) = \{(u_1, u_2) | R(u_1, u_2) = \max_{0 \le p_1, p_2 \le 1} R(p_1, p_2)\}. \tag{A.2}$$

This is (2.1)–(2.4), which is actually a control system with controls (u_1, u_2) relying on the state of the system. Now we look for controls belonging to the strategy map $S(M_A, M_J)$. Then we calculate the derivatives of $S(M_A, M_J)$ to investigate the maximizing controls u_1 and u_2.

$$\frac{\partial R}{\partial u_1} = \frac{M_A e_1 + M_A M_J u_2 (e_1 h_2 - e_2 h_1)}{(1 + h_1 u_1 M_A + h_2 u_2 M_J)^2}, \tag{A.3}$$

$$\frac{\partial R}{\partial u_2} = \frac{M_J (e_2 - M_A u_1 (e_1 h_2 - e_2 h_1))}{(1 + h_1 u_1 M_A + h_2 u_2 M_J)^2}. \tag{A.4}$$

The sign of $\frac{\partial R}{\partial u_1}$ and $\frac{\partial R}{\partial u_2}$ depend on the $e_1h_2 - e_2h_1$.

A tricky point here is that attack rates depend critically on the density of adult and juvenile mussels. That is of $(u_1 = 1, u_2 = 0)$, or $(u_1 = 0, u_2 = 1)$ are feasible as attack rates if the mussel densities are above a certain density. However if M_A, or M_J fall below a certain critical level, theory predicts that the less preferred prey should *also* be attacked, and one might have a situation of $(u_1 = 1, u_2 = 1)$. What we show next, is that if certain parametric restrictions are met, $(u_1 = 1, u_2 = 0)$, or $(u_1 = 0, u_2 = 1)$ are the *only* optimal choices for the crab, irrespective of mussel density.

Lemma A.1. *Consider* (2.1)–(2.4). *If* $e = 0$, *and* $d_1 > \frac{e_2}{h_2}$ *then* $(u_1 = 1, u_2 = 0)$ *is the only optimal choices for the crab. Whereas if* $e = K$, *and* $d_1 > \frac{e_1}{h_1}(u_1 = 0, u_2 = 1)$ *is the only optimal choices for the crab.*

Proof. If $\frac{e_1}{h_1} > \frac{e_2}{h_2}$, $\frac{\partial R}{\partial u_1} > 0$, the maximum of $R(u_1, u_2)$ is thus achieved for $u_1 = 1$. And since the sign of $\frac{\partial R}{\partial u_2}$ does not depend on u_2, it follows if $\frac{\partial R}{\partial u_2} \neq 0$. $R(u_1, u_2)$ will be maximized either with $u_2 = 0$ or $u_2 = 1$. Then we get the strategy map

$$S(M_A, M_J) = \begin{cases} (1,1) & \text{if } M_A < \dfrac{e_2}{e_1h_2 - e_2h_1}, \\ (1,0) & \text{if } M_A > \dfrac{e_2}{e_1h_2 - e_2h_1}, \\ (1,u_2),\ 0 \le u_2 \le 1 & \text{if } M_A = \dfrac{e_2}{e_1h_2 - e_2h_1}. \end{cases} \tag{A.5}$$

Now $M_A^* = \frac{d_1}{e_1 - d_1h_1}$ from the earlier stability calculations. We note,

$$M_A^* = \frac{d_1}{e_1 - d_1h_1} > \frac{e_2}{e_1h_2 - e_2h_1}, \tag{A.6}$$

as long as $d_1 > \frac{e_2}{h_2}$, and if this is enforced $(u_1 = 1, u_2 = 0)$ is the only optimal strategy for the crab.

If $\frac{e_1}{h_1} < \frac{e_2}{h_2}$ in order to maximize $R(u_1, u_2)$, we need $u_2 = 1$. The strategy map will switch to

$$S(M_A, M_J) = \begin{cases} (1,1) & \text{if } M_J < \dfrac{e_1}{e_2h_1 - e_1h_2}, \\ (0,1) & \text{if } M_J > \dfrac{e_1}{e_2h_1 - e_1h_2}, \\ (u_1,1),\ 0 \le u_1 \le 1 & \text{if } M_J = \dfrac{e_2}{e_1h_2 - e_2h_1}. \end{cases} \tag{A.7}$$

Now, $M_J^* = \frac{d_1}{e_2 - d_1h_2}$ from the earlier stability calculations. We note

$$M_J^* = \frac{d_1}{e_2 - d_1h_2} > \frac{e_1}{e_2h_1 - e_1h_2}, \tag{A.8}$$

as long as $d_1 > \frac{e_1}{h_1}$, and if this is enforced $(u_1 = 0, u_2 = 1)$ is again, the only optimal strategy for the crab.

A.2. *Proof of Theorem* 3.2

The Jacobian matrix about (C^*, M_A^*, M_J^*) of system (3.14)–(3.16), without epibiont, is given by

$$J = \begin{bmatrix} 0 & J_{12} & 0 \\ J_{21} & J_{22} & J_{23} \\ 0 & J_{32} & J_{33} \end{bmatrix}, \tag{A.9}$$

where

$$J_{12} = a(e_1 - d_1h_1) - d_1\delta_1, \tag{A.10}$$

$$J_{21} = -\frac{d_1}{e_1}, \tag{A.11}$$

$$J_{22} = -\frac{a(e_1 - d_1h_1)^2 + d_1^2\delta_1h_1 + d_1\delta_1e_1}{e_1(e_1 - d_1h_1)}, \tag{A.12}$$

$$J_{23} = b, \tag{A.13}$$

$$J_{32} = a, \tag{A.14}$$

$$J_{33} = -b. \tag{A.15}$$

The characteristic equation is

$$\lambda^3 + A_2\lambda^2 + A_1\lambda + A_0 = 0, \tag{A.16}$$

with

$$A_2 = -J_{33} - J_{22}, \tag{A.17}$$

$$A_1 = -J_{12}J_{21} + J_{22}J_{33} - J_{23}J_{32}, \tag{A.18}$$

and

$$A_0 = J_{33}J_{21}J_{12}. \tag{A.19}$$

It follows from the Routh–Hurwitz stability criteria that all eigenvalues have negative real part if

$$A_2 > 0, \quad A_0 > 0, \quad A_2A_1 > A_0. \tag{A.20}$$

It is obvious that the first two conditions are always satisfied under feasibility condition (3.20). Furthermore, $A_2A_1 - A_0 > 0$ if $J_{23}J_{32} - J_{22}J_{33} < 0$.

$$J_{23}J_{32} - J_{22}J_{33} = -\frac{bd_1(ad_1h_1^2 - ae_1h_1 + d_1\delta_1h_1 + \delta_1e_1)}{e(e_1 - d_1h_1)} < 0. \tag{A.21}$$

It is enough to solve $bd_1(ad_1h_1^2 - ae_1h_1 + d_1\delta_1h_1 + \delta_1e_1) > 0$, that is, $e_1 - d_1h_1 < \frac{d_1\delta 1}{a} + \frac{d_1\delta_1e_1}{ah_1}$.

Therefore, the system (3.14)–(3.16) is asymptotically stable if

$$\frac{d_1\delta_1}{a} < e_1 - d_1h_1 < \frac{d_1\delta_1}{a} + \frac{d_1\delta_1e_1}{ah_1}. \tag{A.22}$$

A.3. *Proof of Theorem* 3.3

The equilibrium state, of the system (2.1)–(2.4), for the epibiont is $e = K$. At the interior equilibrium state, the parameters $u_1 = 0, u_2 = 1$ and $a(e) = \frac{a}{2}$. Since e will not effect the solution of C, M_A and M_J once u_1, u_2 and $a(e)$ are determined, then it is enough to investigate the following three dimension system with the equilibrium $(C^*, M_A^*, M_J^*) = \left(\frac{1}{2}\frac{ae_2\sqrt{\frac{bd_1}{(e_2-d_1h_2)\delta_1}}}{d_1} - \frac{e_2b}{e_2-d_1h_2}, \sqrt{\frac{bd_1}{(e_2-d_1h_2)\delta_1}}, \frac{d_1}{e_2-d_1h_2}\right)$ when $e = K$.

$$\frac{dC}{dt} = -d_1C + e_2\frac{M_J}{1+h_2M_J}C, \tag{A.23}$$

$$\frac{dM_A}{dt} = bM_J - \delta_1M_A^2, \tag{A.24}$$

$$\frac{dM_J}{dt} = aM_A - bM_J - \frac{M_J}{1+h_2M_J}C. \tag{A.25}$$

The Jacobian matrix about (C^*, M_A^*, M_J^*) is

$$J = \begin{bmatrix} 0 & 0 & J_{13} \\ 0 & J_{22} & J_{23} \\ J_{31} & J_{32} & J_{33} \end{bmatrix}, \tag{A.26}$$

where

$$J_{13} = \frac{1}{2}\frac{\left[a(e_2-d_1h_2)\sqrt{\frac{bd_1}{(e_2-d_1h_2)\delta_1}} - 2bd_1\right](e_2-d_1h_2)}{d_1}, \tag{A.27}$$

$$J_{22} = -2\delta_1\sqrt{\frac{bd_1}{(e_2-d_1h_2)\delta_1}}, \tag{A.28}$$

$$J_{23} = b, \tag{A.29}$$

$$J_{31} = -\frac{d_1}{e_2}, \tag{A.30}$$

$$J_{32} = \frac{a}{2}, \tag{A.31}$$

$$J_{33} = -\frac{1}{2}\frac{a(e_2-d_1h_2)^2\sqrt{\frac{bd_1}{(e_2-d_1h_2)\delta_1}} + 2bd_1^2h_2}{e_2d_1}. \tag{A.32}$$

Since all the parameters are positive, it is obvious that $J_{22} < 0, J_{23} > 0$, $J_{31} < 0, J_{32} > 0$, and $J_{33} < 0$. Under the feasibility condition (3.30), $J_{13} > 0$. And the characteristic equation is given by

$$\lambda^3 + B_2\lambda^2 + B_1\lambda + B_0 = 0, \tag{A.33}$$

where

$$B_2 = -J_{33} - J_{22}, \tag{A.34}$$

$$B_1 = -J_{13}J_{31} + J_{22}J_{33} - J_{23}J_{32}, \tag{A.35}$$

$$B_0 = J_{13}J_{22}J_{31}, \tag{A.36}$$

By Routh–Hurwitz stability criteria, all eigenvalues have negative real part if

$$B_0 > 0, \quad B_1 > 0, \quad B_2 > 0, \quad B_2B_1 - B_0 > 0. \tag{A.37}$$

It is easy to check $B_2 > 0$ and $B_0 > 0$ under the feasility criterion (3.30). $B_1 > 0$ if $J_{22}J_{33} - J_{23}J_{32} > 0$.

$$\begin{aligned} J_{22}J_{33} - J_{23}J_{32} &= \frac{\left(4\sqrt{\frac{bd_1}{\delta_1(e_2-d_1h_2)}}d_1\delta_1h_2 - 2ad_1h_2 + ae_2\right)b}{2e_2d_1} \\ &= \frac{\left(4\sqrt{\frac{bd_1}{\delta_1(e_2-d_1h_2)}}d_1\delta_1h_2 - ad_1h_2 - ad_1h_2 + ae_2\right)b}{2e_2d_1} \\ &= \frac{\left(4\sqrt{\frac{bd_1}{\delta_1(e_2-d_1h_2)}}d_1\delta_1h_2 - ad_1h_2 + a(e_2 - d_1h_2)\right)b}{2e_2d_1}. \end{aligned} \tag{A.38}$$

To make $J_{22}J_{33} - J_{23}J_{32} > 0$, it is enough to show $4\sqrt{\frac{bd_1}{\delta_1(e_2-d_1h_2)}}d_1\delta_1h_2 - ad_1h_2 > 0$, which gives us $e_2 - d_1h_2 < \frac{16bd_1\delta 1}{a^2}$. Furthermore,

$$\begin{aligned} B_2B_1 - B_0 &= J_{13}J_{31}J_{33} - J_{22}^2J_{33} + J_{22}J_{23}J_{32} - J_{22}J_{33}^2 + J_{23}J_{32}J_{33} \\ &= J_{13}J_{31}J_{33} + J_{22}(J_{23}J_{32} - J_{22}J_{33}) + J_{33}(J_{23}J_{32} - J_{22}J_{33}). \end{aligned} \tag{A.39}$$

Since $J_{22} < 0$ and $J_{33} < 0$, $J_{22}J_{33} - J_{23}J_{32} > 0$ implies $B_2B_1 - B_0 > 0$. Thus, the system (2.1)–(2.4) is asymptotically stable if

$$\frac{4bd_1\delta 1}{a^2} < e_2 - d_1h_2 < \frac{16bd_1\delta_1}{a^2}. \tag{A.40}$$

A.4. *Proof of Theorem* 4.1

Now let a, the growth rate of juvenile mussels, as the bifurcation parameter. Therefore, if condition (3.20) holds, $A_0(a_*)$ are always positive. $A_2(a_*) > 0$ if $e_1 - d_1h_1 < \frac{d_1\delta_1}{a} + \frac{d_1\delta_1e_1}{ah_1}$. $\phi(a_*) = A_2(a_*)A_1(a_*) - A_0(a_*) = 0$ if

$$a_* = \frac{f_1}{f_2}, \tag{A.41}$$

where

$$\begin{aligned}
f_1 &= 4b\delta_1^2h_1^5(M_A^*)^7 + (2b^2\delta_1h_1^5 + 20b\delta_1^2h_1^4(M_A^*)^6 + (10b^2\delta_1h_1^4 + 40b\delta_1^2h_1^3)(M_A^*)^5\\
&\quad + (4C^*b\delta_1h_1^3 + 20b^2\delta_1h_1^3 + 2C^*\delta_1e_1h_1^2 + 40b\delta_1^2h_1^2)(M_A^*)^4\\
&\quad + (C^*b^2h_1^3 + 12C^*b\delta_1h_1^2 + 20b^2\delta_1h_1^2 + 4C^*\delta_1e_1h_1 + 20b\delta_1^2h_1)(M_A^*)^3\\
&\quad + (3C^*b^2h_1^2 + 12C^*b\delta_1h_1 + 10b^2\delta_1h_1 + 2C^*\delta_1e_1 + 4b\delta_1^2)(M_A^*)^2\\
&\quad + ((C^*)^2bh_1 + 3C^*b^2h_1 + (C^*)^2e_1 + 4C^*b\delta_1 + 2b^2\delta_1)M_A^* + (C^*)^2b + C^*b^2,\\
f_2 &= b(M_A^*h_1 + 1)^3(2(M_A^*)^3\delta_1h_1^2 + b(M_A^*)^2h_1^2 + 4(M_A^*)^2\delta_1h_1 + 2bM_A^*h_1\\
&\quad + 2M_A^*\delta_1 + C^* + b),
\end{aligned} \tag{A.42}$$

and C^*, M_A^* are given by (3.17) and (3.18).

Furthermore, it is easy to verify that

$$\begin{aligned}
\frac{d\phi(a)}{da}|_{a=a_*} &= -\frac{(b(M_A^*)^3h_1^3 + 3b(M_A^*)^2h_1^2 + 3bM_A^*h_1 + b)(2(M_A^*)^2\delta_1h_1^2}{(M_A^* + 1)^5}\\
&\quad - \frac{(bh_1^2 + 4\delta_1h_1)(M_A^*)^2 + (2bh_1 + 2\delta_1)M_A^* + C^* + b)}{(M_A^* + 1)^5}\\
&< 0 \neq 0.
\end{aligned} \tag{A.43}$$

A.5. *Proof of Theorem* 5.4

The Hamiltonian of the system is given by

$$H = M_A + M_J - \frac{1}{2}u_1^2 + \lambda_1C' + \lambda_2M_A' + \lambda_3M_J'. \tag{A.44}$$

We use the Hamiltonian to find a differential equation of the adjoint $\lambda_i, i = 1, 2, 3$.

$$\begin{aligned}
\lambda_1'(t) &= -\lambda_1\left(-d_1 + \frac{M_Ae_1u_1 + M_Je_2u_2}{M_Ah_1u_1 + M_Jh_2u_2 + 1}\right)\\
&\quad + \frac{\lambda_2u_1M_A}{M_Ah_1u_1 + M_Jh_2u_2 + 1} + \frac{\lambda_3u_2M_J}{M_Ah_1u_1 + M_Jh_2u_2 + 1},\\
\lambda_2'(t) &= -\lambda_1\left(\frac{e_1u_1C}{M_Ah_1u_1 + M_Jh_2u_2 + 1} - \frac{(M_Ae_1u_1 + M_Je_2u_2)Ch_1u_1}{(M_Ah_1u_1 + M_Jh_2u_2 + 1)^2}\right)\\
&\quad - \lambda_2\left(-2\,\delta_1M_A - \frac{u_1C}{M_Ah_1u_1 + M_Jh_2u_2 + 1}\right.\\
&\quad \left. + \frac{{u_1}^2M_ACh_1}{(M_Ah_1u_1 + M_Jh_2u_2 + 1)^2}\right)\\
&\quad - \lambda_3\left(a/2 + \frac{u_2M_JCh_1u_1}{(M_Ah_1u_1 + M_Jh_2u_2 + 1)^2}\right) - 1,
\end{aligned}$$

$$\begin{aligned}\lambda_3'(t) = &-\lambda_1\left(\frac{e_2u_2C}{M_Ah_1u_1+M_Jh_2u_2+1}-\frac{(M_Ae_1u_1+M_Je_2u_2)Ch_2u_2}{(M_Ah_1u_1+M_Jh_2u_2+1)^2}\right)\\ &-\lambda_2\left(b+\frac{u_1M_ACh_2u_2}{(M_Ah_1u_1+M_Jh_2u_2+1)^2}\right)\\ &-\lambda_3\left(-b-\frac{u_2C}{M_Ah_1u_1+M_Jh_2u_2+1}+\frac{{u_2}^2M_JCh_2}{(M_Ah_1u_1+M_Jh_2u_2+1)^2}\right)-1,\end{aligned} \tag{A.45}$$

with the transversality condition gives as

$$\lambda_1(T)=\lambda_2(T)=\lambda_3(T)=0. \tag{A.46}$$

By solving

$$\begin{aligned}0=\frac{\partial H}{\partial u_1} =&\lambda_1\left(\frac{M_Ae_1C}{M_Ah_1u_1+M_Jh_2u_2+1}-\frac{(M_Ae_1u_1+M_Je_2u_2)CM_Ah_1}{(M_Ah_1u_1+M_Jh_2u_2+1)^2}\right)\\ &+\lambda_2\left(-\frac{M_AC}{M_Ah_1u_1+M_Jh_2u_2+1}+\frac{u_1{M_A}^2Ch_1}{(M_Ah_1u_1+M_Jh_2u_2+1)^2}\right)\\ &+\lambda_3\frac{u_2M_JCM_Ah_1}{(M_Ah_1u_1+M_Jh_2u_2+1)^2}-u_1,\\ 0=\frac{\partial H}{\partial u_2} =&\lambda_1\left(\frac{M_Je_2C}{M_Ah_1u_1+M_Jh_2u_2+1}-\frac{(M_Ae_1u_1+M_Je_2u_2)CM_Jh_2}{(M_Ah_1u_1+M_Jh_2u_2+1)^2}\right)\\ &+\lambda_2\frac{u_1M_ACM_Jh_2}{(M_Ah_1u_1+M_Jh_2u_2+1)^2}\\ &+\lambda_3\left(-\frac{M_JC}{M_Ah_1u_1+M_Jh_2u_2+1}+\frac{u_2{M_J}^2Ch_2}{(M_Ah_1u_1+M_Jh_2u_2+1)^2}\right).\end{aligned} \tag{A.47}$$

u_{1_2} and u_{2_2} equal to

$$\begin{aligned}u_{1_2}=&\frac{e_2\lambda_1-\lambda_3}{M_A(e_1h_2\lambda_1-e_2h_1\lambda_1+h_1\lambda_3-h_2\lambda_2)},\\ u_{2_2}=&\frac{w_1}{w_2},\end{aligned} \tag{A.48}$$

where

$$\begin{aligned}w_1 = &CM_A{}^2e_1{}^3h_2{}^3\lambda_1{}^3-3CM_A{}^2e_1{}^2e_2h_1h_2{}^2\lambda_1{}^3+3CM_A{}^2e_1e_2{}^2h_1{}^2h_2\lambda_1{}^3\\ &-CM_A{}^2e_2{}^3h_1{}^3\lambda_1{}^3+3CM_A{}^2e_1{}^2h_1h_2{}^2\lambda_1{}^2\lambda_3-3\,CM_A{}^2e_1{}^2h_2{}^3\lambda_1{}^2\lambda_2\\ &-6CM_A{}^2e_1e_2h_1{}^2h_2\lambda_1{}^2\lambda_3+6\,CM_A{}^2e_1e_2h_1h_2{}^2\lambda_1{}^2\lambda_2+3\,CM_A{}^2e_2{}^2h_1{}^3\lambda_1{}^2\lambda_3\\ &-3CM_A{}^2e_2{}^2h_1{}^2h_2\lambda_1{}^2\lambda_2+3\,CM_A{}^2e_1h_1{}^2h_2\lambda_1\lambda_3{}^2-6\,CM_A{}^2e_1h_1h_2{}^2\lambda_1\lambda_2\lambda_3\\ &+3CM_A{}^2e_1h_2{}^3\lambda_1\lambda_2{}^2-3\,CM_A{}^2e_2h_1{}^3\lambda_1\lambda_3{}^2+6\,CM_A{}^2e_2h_1{}^2h_2\lambda_1\lambda_2\lambda_3\end{aligned}$$

$$
\begin{aligned}
&- 3CM_A{}^2e_2h_1h_2{}^2\lambda_1\lambda_2{}^2 + CM_A{}^2h_1{}^3\lambda_3{}^3 - 3\,CM_A{}^2h_1{}^2h_2\lambda_2\lambda_3{}^2 \\
&+ 3CM_A{}^2h_1h_2{}^2\lambda_2{}^2\lambda_3 - CM_A{}^2h_2{}^3\lambda_2{}^3 - e_1e_2h_2{}^2\lambda_1{}^2 + e_1h_2{}^2\lambda_1\lambda_3 \\
&+ e_2h_2{}^2\lambda_1\lambda_2 - h_2{}^2\lambda_2\lambda_3, \\
w_2 = {}& M_Jh_2^2(e_1e_2h_2\lambda_1^2 - e_2^2h_1\lambda_1^2 - e_1h_2\lambda_1\lambda_3 + 2\,e_2h_1\lambda_1\lambda_3 - e_2h_2\lambda_1\lambda_2 - h_1\lambda_3^2 \\
&+ h_2\lambda_2\lambda_3). \qquad \text{(A.49)}
\end{aligned}
$$

So that the optimal controls for $J_2(u_1, u_2)$ is

$$
\begin{aligned}
u_1^* &= \min(1, \max(0, u_{1_2})), \\
u_2^* &= \min(1, \max(0, u_{2_2})).
\end{aligned} \qquad \text{(A.50)}
$$

A.6. *Proof of Theorem* 5.6

The Hamiltonian of our problem is given by

$$
H = M_A + M_J - \frac{1}{2}\delta_1^2 + \lambda_1 C' + \lambda_2 M_A' + \lambda_3 M_J'. \qquad \text{(A.51)}
$$

The differential equations for $\lambda_1'(t), \lambda_2'(t)$ and $\lambda_3'(t)$, are standard and are derived as in Theorem 5.4.

The transversality condition is

$$
\lambda_1(T) = \lambda_2(T) = \lambda_3(T) = 0. \qquad \text{(A.52)}
$$

Considering $\frac{\partial H}{\partial \delta_1} = -M_A{}^2\lambda_2 - \delta_1$, we derive the optimal control for $J_3(\delta_1)$

$$
\delta_1^* = \max(0, -M_A^2\lambda_2). \qquad \text{(A.53)}
$$

□

A.7. *Numerical explorations of bifurcations of alternate models*

In the case $e = K$, we do not see a Hopf bifurcation numerically. It is worthwhile considering certain alternate models for the epibiont dynamics as future work. We motivate this via considering the following model:

$$
\begin{aligned}
\frac{dC}{dt} &= -d_1C + e_1u_1(e)\frac{M_A}{1 + h_1u_1(e)M_A + h_2u_2(e)M_J}C \\
&\quad + e_2u_2(e)\frac{M_J}{1 + h_1u_1(e)M_A + h_2u_2(e)M_J}C, \qquad \text{(A.54)}
\end{aligned}
$$

$$
\frac{dM_A}{dt} = bM_J - \delta_1M_A^2 - u_1(e)\frac{M_A}{1 + h_1u_1(e)M_A + h_2u_2(e)M_J}C, \qquad \text{(A.55)}
$$

$$
\frac{dM_J}{dt} = a(e)M_A - bM_J - u_2(e)\frac{M_J}{1 + h_1u_1(e)M_A + h_2u_2(e)M_J}C, \qquad \text{(A.56)}
$$

$$
\frac{de}{dt} = b_1e\left(1 - \frac{e}{k_1M_A + k_2}\right). \qquad \text{(A.57)}
$$

where

$$u_1(e) = \frac{K-e}{K}, \quad u_2(e) = \frac{e}{K}, \quad a(e) = a\left(\frac{K-\frac{e}{2}}{K}\right), \quad K = k_1 M_A + k_2, \quad \text{(A.58)}$$

with positive initial conditions $C(0) = C_0, M_A(0) = M_{A0}, M_J(0) = M_{J0}, e(0) = e_0$. These responses are for the range $0 \leq e \leq K$.

The only change here to crab–mussel system (A.54)–(A.57) is that we assume the carrying capacity of the epibiont is density dependent, and depends primarily on the adult mussel density that is $K = K = k_1 M_A + k_2$. Here, k_2 represents alternate substrate that the epibiont can grow on.

The four-dimensional system has 11 parameters with four dependent variables. The following parameters are used in numerical simulations:

$$\begin{aligned} &e_1 = 0.8, \quad e_2 = 0.5, \quad d_1 = 0.4, \quad a = 4, \quad b_1 = 2, \quad b = 0.5, \\ &h_1 = 2, \quad h_2 = 1, \quad \delta_1 = 0.2, \quad k_1 = 0.1, \quad k_2 = 0.3. \end{aligned} \quad \text{(A.59)}$$

The system evolve the stable limit cycles for parameter set (A.59). Time series for all species is shown in Fig. A.1(a), while limit cycles in 2D phase space are shown in Figs. A.1(b), A.2(a) and A.2(b). To observe more qualitative behavior of the model, one-parameter bifurcation diagram is drawn with respect to parameter d_1 and parameter a in the figures. A supercritical Hopf bifurcation occurs at $d_1 = 0.3567$ which emanates stable limit cycles. There is another supercritical hopf bifurcation at $d_1 = 0.444$. Between these two Hopf bifurcations, the model has periodic solutions. After second Hopf bifurcation point model has stable solutions, crab populations are going to extinct. The dynamics is shown in one-parameter bifurcation diagram in Fig. A.3(a). The qualitative dynamics has been also obtained for the range of parameter a drawn in the Fig. A.3(b). Initially, for low parameter value $a < 1.265$, the crab population is too low but as parameter a increases,

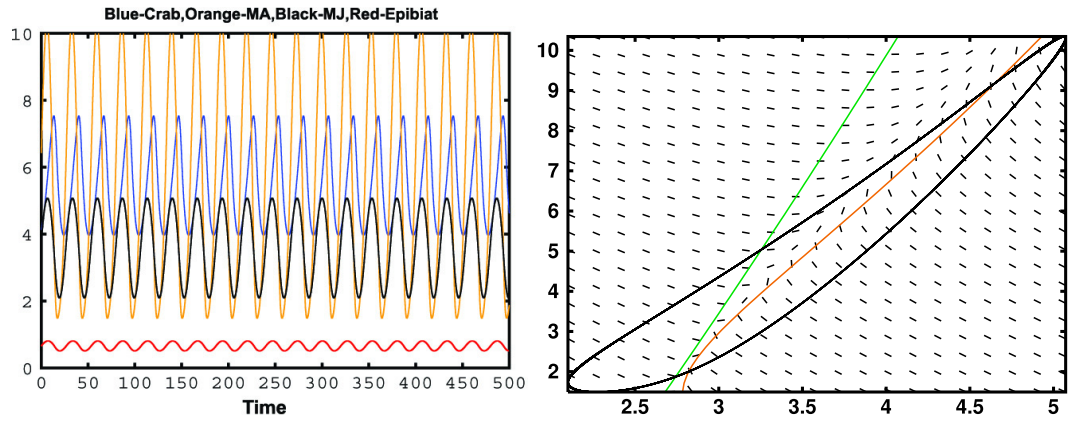

(a) The biomasses of all species exhibited the periodic coexistence against the time series is shown for parameter set (A.59).

(b) A stable limit cycle in the two-dimensional phase space M_A and M_J for parameter set (A.59).

Fig. A.1. Time-series and limit cycle in the 2D phase space plot.

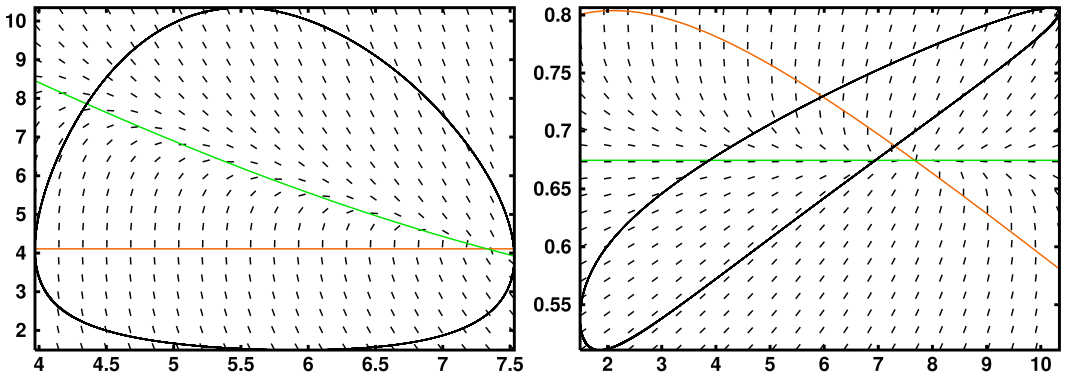

(a) A stable limit cycle in the two-dimensional phase space C and M_J for parameter set (A.59).

(b) A stable limit cycle in the two-dimensional phase space E and M_j for parameter set (A.59).

Fig. A.2. Stable limit cycle in the 2D phase space plot.

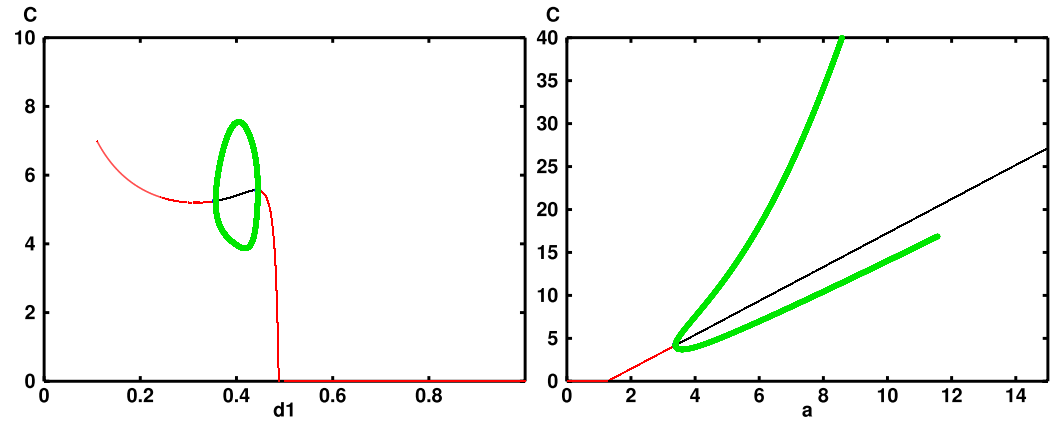

(a) One-parameter bifurcation diagram with respect to parameter d_1.

(b) One-parameter bifurcation diagram with respect to parameter a.

Fig. A.3. One-parameter bifurcation diagrams to depict stablilty, Hopf bifurcation point and periodic solutions with respect to parameter set (A.59).

model exhibits stable coexistence. Further, it undergoes through supercritical Hopf bifurcation at parameter $a = 3.386$ which emanates stable limit cycles (green filled circle).

The parameter region has been obtained by drawing two-parameter (a, d_1) bifurcation diagram in Fig. A.4(a). The parameter region for which one species goes extinct is shown in shaded region (extreme left), the region for which stable coexistence is possible is shown in red and the region for which periodic solution is possible is shown in blue color in Fig. A.4(a). Another two-parameter (d_1, δ) bifurcation diagram is drawn in Fig. A.4(b). The parameter region for which stable coexistence occurs and region for which periodic solution is possible is depicted in Fig. A.4(b).

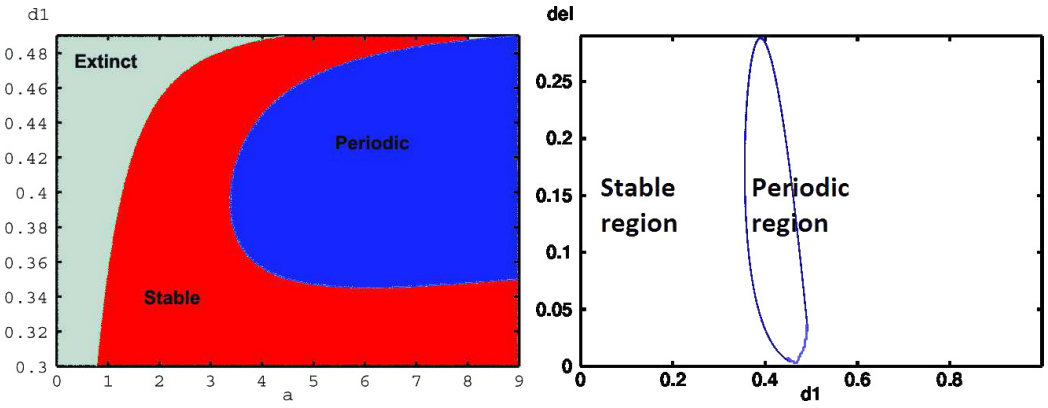

(a) Two-parameters (a, d_1) bifurcation diagram with respect to parameter set (A.59).

(b) Two-parameters (d_1, δ) bifurcation diagram with respect to parameter set (A.59).

Fig. A.4. Two-parameter bifurcation diagrams to depict parameter region for the stable coexistence and periodic coexistence with respect to parameter set (A.59).

As shown by these bifurcation graphs, model has periodic solutions for biologically feasible choice of parameters and one can find the Hopf bifurctaion point for each of the parameters used in the model.

These results show that a Hopf bifurcation is possible, if one considers a density-dependent carrying capacity for the epibiont. These results are robust in nature as different sets of parameters will yield the same qualitative behavior. The periodicity in the system is beneficial for harvesting and coexistence of all the species involved.